X-601-74-349

PREPRINT

NASA TM X- 70823

ORBITAL FLUX INTEGRATIONS: PARAMETER VALUES FOR EFFECTIVE COMPUTER TIME REDUCTIONS

E. G. STASSINOPOULOS

NOVEMBER 1974

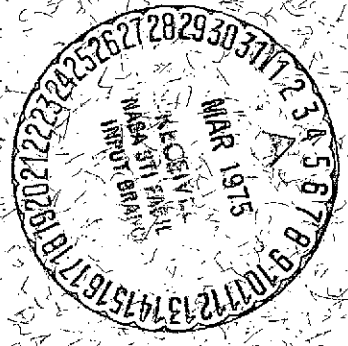

GSFC

GODDARD SPACE FLIGHT CENTER

GREENBELT, MARYLAND

For information concerning availability
of this document contact:

Technical Information Division, Code 250
Goddard Space Flight Center
Greenbelt, Maryland 20771

(Telephone 301-982-4488)

ORBITAL FLUX INTEGRATIONS:

Parameter Values for Effective Computer Time Reduction

E. G. Stassinopoulos

NASA-Goddard Space Flight Center
Sciences Directorate
National Space Science Data Center

November 1974

Goddard Space Flight Center
Greenbelt, Maryland 20771

Foreword

In order to improve computer utilization and reduce the cost of orbital flux integrations, the effects of integration parameters "duration" (T) and "stepsize" (Δt) on integration results were investigated. Over given ranges of T and Δt, and within specified acceptable accuracy restraints, optimal values of these parameters were established for circular subsynchronous trajectories, in terms of the variables altitude (h) and inclination(i).

It is shown that above a certain statistically important value, duration is independent of both h and i; that is, the integration results are virtually unaffected by increases in T at any h or i, for any given Δt.

It is also shown that stepsize has a "relative" altitude dependence; that is, at any given altitude, regardless of duration or inclination, the integration results remain nearly constant for a substantial range of Δt, but they will vary appreciably whenever Δt is increased beyond some specific value, characteristic for that altitude level. Stepsize, however, is not a function of inclination, because the fluxes obtained with different Δt's at each tested inclination did not vary significantly, regardless of altitude or duration.

Finally, the substantial savings in computer time, realized by minimizing T and maximizing Δt over their respective investigated ranges and for the specified accuracy restraints, are presented and the possibilities

are discussed to achieve still greater savings by further relaxing accuracy restrictions while not exceeding the minimum model-associated uncertainty factors of the environments.

Contents

List of Tables

List of Figures

Definitions:

Introduction

T = duration, length of lfight time interval considered in an orbital flux integration (hours)

Δt= stepsize, time increment of integration (minutes)

h = orbit altitude above sea level (km)

i = orbit inclination (prograde) (degrees)

Precession

P = precession of orbit plane (degrees)

τ = orbit period (hours)

k = proportionality constant = rotational speed of earth (degrees/hour)

c = conversion factor (seconds/hour)

r_e= equatorial radius of earth (km)

μ = gravitational constant (km^3/sec^2)

Duration and Stepsize

D = simple flux deviations over Δt; based on a comparison of results obtained with Δt_{max} and Δt_{min} for a constant h,i, and T.

D^*= transverse flux deviations over Δt and T; based on a comparison of results obtained with the highest density (T_{max}, Δt_{min}) and the lowest density (T_{min}, Δt_{max}) of points available for a constant h and i.

D_T^*= correlated flux deviations over T; based on a comparison of results obtained with the highest density (T_{max}, Δt_{min}) and lower densities (T_{other}, Δt_{min}) of points available for a constant h, i, and Δt.

$N(T, \Delta t)$ = number of actually evaluated flight path positions (trajectory points)

$\overline{\tau}_I(h;T, \Delta t)$ = actual computer running time averaged over inclination: combined CPU and I/O values of the execution step.

R_p = ratio of $N(T, \Delta t)$'s of transverse comparisons

$\overline{R}_{t_I}$ = ratio of $\overline{\tau}_I(T, \Delta t)$'s of transverse comparisons

d = conversion factor (min/hour)

INTRODUCTION

Near-Earth space missions are routinely exposed to hazards deriving from various types of space radiation, as for example: galactic cosmic rays, energetic solar protons, Van Allen belt particles, etc. It is often important for effective mission planning purposes to have available advance information as to the severity of the expected radiation hazard, especially in order to calculate shielding requirements for man and equipment (weight problem), and in order to establish lifetimes and degradation of experiments, satellite components, power supply, etc.

Predictions of vehicle encountered trapped particle fluxes are usually obtained from Orbital Flux Integration (o.f.i.) processes, frequently performed over arbitrary lengths of flight-time intervals T and with arbitrary time increments Δt. However, both quantities affect not only precious computer time but also determine the precision of the calculated data. Thus, very short T's and/or very large Δt's may introduce substantial errors into the flux predictions while long T's and/or very small Δt's can be excessive and wasteful on computer time. Conceivably, an optimization of the variables "T" and "Δt" in terms of orbit altitude and inclinations may produce considerable savings in computer time while still insuring the accuracy of the results.

This report describes the procedure and presents the conclusions of an effort to approximate, within a given range of T and Δt, optimal values of these parameters in regards to computer time, with the stipulation that the results obtained for a fixed inclination and altitude

with the smallest number of points may not vary by more than 20% from the results obtained at the same i and h with the largest number of points. That is, within the range of interest, only those combinations of T and Δt values will be considered optimal, that minimize the number of points for which the error in the orbit integrated fluxes does not exceed 20%. The error limit was determined by taking one fifth of the minimum model-associated uncertainty factor of the environments, which is generally a factor of two or greater for both species of particles.

In the evaluation of the two parameters T and Δt, only circular trajectories were considered. Elliptical flight paths require special treatment and will be discussed in a separate report at a later date.

Orbital flux integrations were performed with the "UNIFLUX" system (Stassinopoulos and Gregory, 1974), described briefly in the Appendix, at six altitude levels and for four inclinations each, with three different stepsizes in every case, and for durations extending to 96 hours for the highest altitudes. Table 1 lists the values of some relevant parameters and variables. Table 2 indicates the number of samplings contained in trajectories with duration T and stepsize Δt for selected values of these variables.

Although the parameter evaluation presented in this analysis is based exclusively on integral proton and electron fluxes of energies $E > 5.$Mev and $E > .5$Mev respectively, the calculations and the comparisons were actually performed for several energies. It was found that the comparison results were about the same and that the conclusions were valid for all investigated energies of both particle species. That is, no special considerations are necessary for different energy thresholds.

It should be noted that no B-L calculations are performed in the UNIFLUX system.

The environment models used in the flux calculations are the AE5 for inner zone electrons (Teague and Vette, 1972), the AE4 for outer zone electrons (Singley and Vette, 1972) and the AP6 for high energy protons (Lavine and Vette, 1969).

Data, discussions, and conclusions apply only to space missions in circular orbits and of long durations (>15 revolutions); they are not valid for short sorties, parking orbits, transfer ellipses, or eccentric trajectories. Neither are they valid for L-band* accumulations**. L-band accumulations have not been considered in this work because of the very small interest in them and because of their limited usefulness.

---

*L is McIlwain's (1961) magnetic shell parameter, which is used to label field lines, to order trapped particles, and to construct environment models; it is defined as the geocentric distance to the point where a line of force intersects the geomagnetic equator.

**L-band accumulations are the summations of time related fluxes obtained, for a given L-range, in discrete L intervals or bands.

APPARENT ORBIT PRECESSION

In the context of this paper, "longitudinal orbit precession" is the apparent westward drift of the orbit plane in reference to the rotating geoid. The precession P in degrees is proprotional to the orbit period τ in hours.

$$P = k\tau \quad \text{(degrees)} \tag{1}$$

where the proportionality factor k is the rotational speed of the Earth in degrees per hour. Since τ is a function of trajectory altitude h, equation (1) can be written equivalently as

$$P = \frac{2k\pi}{c} \sqrt{\frac{(h+r_e)^3}{\mu}} \tag{2}$$

where the conversion factor c = 3600 sec/hr, the equatorial Earth radius r_e = 6378.165 km, and the constant μ = 3.986032 X 10^5 km^3/sec^2. Values of P versus h are given in Figure 1.

With the exception of very short-term missions (flight duration T less than half a day), precession should have no effect on mission integrated fluxes and, as will be shown in a subsequent section, a flight duration of one day (T = 24 hours) is fully sufficient to insure good integration results for most subsynchronous altitudes up to about 32,000 kilometers. Synchronous trajectories will be discussed in a special paper.

The old belief that at low altitudes precession may cause the trajectory to miss (skip, not sample) important parts of the trapped particle radiation belts, particularly the highest intensity regions of the South Atlantic Anomaly, shown in Figures 2 and 3 as the "10^5" contours

for electrons with energies E >.5 MeV at the 300 and 1000 km altitude levels, is unfounded because in the critical low altitude domain (300 - 1000 km) these intensity areas increase more rapidly in size when height is raised than does precession. This holds true for all energies. Incidentally, protons follow the same pattern.

At higher altitudes, where the multipole nature of the non-centered geomagnetic field and its anomalies rapidly disappear and the field approaches dipolar symmetry, precession is of no consequence because the particle gradients with L are much smaller.

DURATION AND STEPSIZE

The data used in this analysis were obtained from a total of 168 orbital flux integration runs.

The smallest unit of duration investigated was one day, the largest four days. Shorter time intervals were of no concern to this study. The possibility, however, that T's of less than 24 hours could produce acceptable results for some particular orbits, cannot be ruled out.

As indicated in Table 3, several durations were used at all but the very low altitude levels, for all inclinations. In every case three stepsizes were tried.

Figures 4 and 5 depict, for electrons and protons respectively, absolute percentage-flux-deviations ($|D|$ %) versus altitude for the four selected inclinations and the indicated durations, where the fluxes obtained with the smallest stepsize are compared to those of the largest. The stepsizes and durations are given in Table 3. According to the stipulated accuracy requirement, the apparent improvements in some of the results for the longer durations, are completely insignificant and meaningless; ranging from a small fraction of one percent to a maximum of 5%, these improvements lie totally in the "noise" area of the flux data, which it will be remembered, are no better than a factor of 2, to begin with. A comprehensive comparison of minimum model-uncertainty-factors to duration and stepsize deviations appears in a subsequent section.

Interestingly, the largest deviations of the T = 24 hour runs for the electrons and protons at h = 400 and h = 1000 km, due

entirely to the stepsize variation, shrink with increasing altitude and with greater stepsize variations. One might have expected the opposite to happen, since duration remained constant. A possible reason for the larger D's at the low altitudes, for both species of particles, may be the high intensity gradients of the inner trapping boundaries (more relevant comments on page 8).

The 24-hour curves further indicate that above 4000 km and up to almost synchronous altitudes, the deviations lie well within the acceptable error limit. Therefore, it is safe to use this smallest of the tested durations in the entire investigated h domain. As for the electrons, the data presented amply supports this proposal. Since energetic protons do not extend to synchronous altitudes, longer durations are of no concern. In regards to the protons, some related questions are discussed in a following paragraph.

Transverse flux deviations D^{*} obtained for a given orbit (fixed altitude and inclination) from a comparison of fluxes calculated with the smallest number of points, F(T=min, Δt=max), to fluxes calculated with the largest number of points, F(T=max, Δt=min), per altitude level per inclination, are shown in Figures 6 and 7, for electrons and protons respectively. For this comparison, data obtained with the durations and stepsizes indicated in Table 3 by circles around the Δt values were selected. The maximum cross-correlated deviation for electrons occurs at h = 30,000 km when the F_e(T=96, Δt=3) is compared to the F_e(T=24, Δt=9) for all inclinations (0^{o} = 8.6%, 30^{o} = 13.6%, 60^{o} = 12.8%, 90^{o} = 14.8%). The worst case for protons occurs at h = 16,000 km but with additional occurrences at h = 400 km for the case i = 0^{o}, and h = 4000 km for all inclinations.

Particularly interesting is the equatorial proton curve at 16,000 km, jumping to the highest deviation (8.4%) encountered for these particles in the tests. When the respective data is checked in detail, it becomes apparent that this unusual rise in deviation: (1) is not related to a change in Δt (the individual results are totally insensitive to stepsize variation), and (2) appears in all three sets of runs (one set for each Δt) where stepsize was kept constant but duration was varied from 24 to 96 hours. Evidently, this rise is not experienced by the inclined orbits. The reason for this phenomenon may be that the equatorial trajectory is skimming the very edge of the 5 MeV proton trapping region, which extends slightly past 16,000 km, and as duration is increased, a better statistical average is obtained. If altitude is further raised, no more 5 MeV protons will be encountered. This very special case is the only exception to the rule about duration. It will not be taken into account.

In this regard, it has been argued that at or near the proton trapping boundary larger durations and/or smaller stepsizes would improve o.f.i. results. This may be true but it is of marginal importance because at the trapping boundary the particle intensities are insignificantly small and, in most practical cases, do not contribute at all to the four significant figures with which the fluxes of a standard o.f.i. calculation are given. Furthermore, the location of this boundary, on or off the geomagnetic equator, is a function of the particle energy, among other things; on the equator it lies at about L=3.6 Earth radii for the $E > 5$ MeV protons and at about L=2.5 Earth radii for $E > 100$ MeV protons.

To take these details into account and to design programs around them, capable of handling all kinds of circular and elliptical trajectories, would be inefficient and expensive in comparison to the effected improvement in the results; the same can be said for the equivalently wasteful approach of varying duration and stepsize in such a way as to achieve a longer and denser environment sampling.

In either case, a very small fractional gain in accuracy is really trivial in view of the size of the minimum model-associated uncertainty factor of the environments.

The same argument applies also to the inner (low altitude) boundary, only that there the intensity gradient is much steeper and the energy dependent boundary locations lie much closer together. These enhanced conditions may affect the o.f.i. results of very low altitude (400 km) circular missions (elliptical trajectories with very low perigee fall into the category discussed in the previous paragraph).

Anyhow, the altitude regime below 400 km is of small interest and importance to this study because, with very few exceptions, it is not frequented by circular missions due to the rapidly increasing atmospheric drag effect experienced by spacecraft at these heights.

At this time, it is important to remember that except the one special case for protons and the 30,000 km altitude for electrons, all these so-called "maximum deviations" are less than 5% while the uncertainties inherent in the environment models used in the calculations are at least a factor of two. In this perspective, the deviations obtained in the tests are truly insignificant, even the exceptional ones. See Figure 8 for a proportional presentation of maximum deviations

versus model-uncertainty factor. This would of course allow the use of still larger increments or shorter intervals, further decreasing the number of points processed and further reducing computer time. However, it is suggested not to increase stepsizes or reduce duration beyond values which would produce deviations of 30% or greater.

The trends in the curves on Figures 6 and 7 between 4000 and 16000 km imply some altitude dependence of the 0^{o}, 60^{o}, and 90^{o} inclinations for the electrons, a very strong altitude dependence of the $i = 0^{o}$ curve for the protons (on the same curve also observed at 400 km; reason explained in a preceeding paragraph), and a rather weak dependence of the $i = 60^{o}$ proton curve. Above 16000 km (electrons only), curves of all inclinations display a sharp rise with altitude.

In regards to an old argument, that polar orbits supposedly need smaller stepsizes than equatorial orbits in order to yield equally good results, it seems to have been resolved by the present study; no evidence was found in the data to support that contention. On the contrary, of the fourteen polar cases tested, each with three different stepsizes for a total of 42 runs, none indicated any abnormal, excessive, or plainly significant deviation in the integrated fluxes, not even when the Δt was tripled or quintupled. Over all, no one particular inclination tested did stand out in any way by producing consistently either better or worse results, for any stepsize. Figure 9 shows the stepsize deviation of polar and equatorial orbits in comparison to the minimum model-uncertainty-factor of 2.

When the data were ordered so as to determine the dependence of $|D|$% on T, Figures 11 - 14, it became apparent that longer durations

do not necessarily produce better results. Specifically, in all cases listed in Table 4 the simple deviations did not improve when T was increased.

Another approach to evaluate the T dependence of the o.f.i. results is by defining the quantity D_T^* (correlated deviation) for constant inclination and altitude:

$$D_T^* = \frac{F(T, \Delta t) - F(T_{other}, \Delta t)}{F(T, \Delta t)} \qquad (3)$$

This permits a data comparison based on duration alone. It is assumed that in the limit as T approaches infinity and Δt approaches zero, the $F(T, \Delta t)$ would have the greatest possible accuracy and that D_T^* would become smaller as values of T_{other} would approach T. The available closest approximation to this formula was used in the evaluation that follows:

$$D_T^* = \frac{F(T_{max}, \Delta t_{min}) - F(T_{other}, \Delta t_{min})}{F(T_{max}, \Delta t_{min})} \qquad (4)$$

The results are discussed in the subsequent paragraphs. Again it should be remembered when talking about differences between D_T^*'s, that most deviations are really insignificantly small and that none exceed the specified error limit.

Figure 15 shows the absolute "correlated deviations" for electrons with energies $E > .5$ Mev and Figure 16 for protons with $E > 5.$ Mev, plotted versus comparison range, where range number 1 always pertains to a comparison of T_{max} to T_{min}. In this comparison, the latter quantity has always the same value of 24 hours at all altitude levels, all inclinations, in contrast to T_{max}, which has different values at different

altitude levels; however, at any given height, T_{max} is the same for all inclinations, as indicated in Table 3. Range number 2, if available, is a comparison of the maximum-duration result to the result obtained from the T_{min} + 24 (hours) run; similarly, range number 3 compares the T_{max} to the T_{min} + 48 (hours) results.

On both figures, the deviations of the i=90° results at 4000 km increased, contrary to expectations, when T_{other} was extended from 24 to 48 hours, that is, going from range 1 to range 2. At the same altitude, the results for i=60° remained almost constant while for i=30° and i=0° the D_T^*'s improved markedly.

A more complex situation exists at the 16000 km altitude level, where three ranges are available for comparison. The electrons at this height showed substantial improvement for the two high inclinations (i=60°, 90°), especially going from range 2 to range 3, but indicate no significant improvement for the two low inclinations (i=0°, 30°) at these ranges. The protons display a perplexing reversal at i=60° and i=90°: whereas almost no improvement is evident when comparing range #1 to range #3, the deviations in range #2 drop by about two orders of magnitude. No explanation can be given for this inversion. It appears as if a cyclic phase-effect were associated with duration, having a half-cycle of about 48 hours.

At 30000 km (electrons only) no range #2 data is available. In the comparison of range #1 to range #3, all inclinations show some small improvements.

The D_T^*'s of a fixed range are also plotted as functions of inclination in Figures 17-20 for the electrons and in Figures 21-23 for the protons,

each Figure corresponding to one of the investigated altitude levels. Some general observations on these plots:

a) the dependence of D_T^* on inclination is a function of particle species, range number, and altitude;

b) deviations of a higher range will usually have a smaller value than those of a lower range; and

c) polar orbits have as a rule higher deviations than equatorial orbits.

There are of course exceptions to items (b) and (c). For (b) these imply that longer durations do not necessarily always produce better results.

Since in no instance did the deviations exceed the specified error limit, even for the transverse comparisons presented in Figures 6 and 7, it is suggested that for the purpose of orbital flux integrations, the smallest tested time interval (T=24 hours) be adopted as a uniform, standard flightpath duration for all circular subsynchronous trajectories.

In conclusion, a range of optimum Δt's per altitude is presented in Figure 10, where the lower value produces an average deviation of less than 10%, and the higher value an average deviation of less than 20%.

A diagonal line in the graph expresses the functional relationship of a continuous optimum stepsize in altitude

$$\Delta t = m \log h + d \tag{5}$$

where

$$m = \frac{\partial(\Delta t)}{\partial(\log h)} = 3.4767, \qquad d = -6.0 \tag{6}$$

This is then used to determine altitude intervals over which a mean, discrete Δt would be valid. For the purpose of simplicity and practicality, we now propose the stepsizes indicated at the top of the shaded areas as standard Δt's for the altitude interval covered by these areas.

COMPUTER TIME

It is obvious that by minimizing duration and by maximizing stepsize one also minimizes computer time. For the combination of parameters and variables considered in the transverse comparisons, the ratio R_p of actually evaluated flight-path positions N (i.e., the number of integration steps or trajectory points) is defined as

$$R_p = \frac{N(T_{max}, \Delta t_1)}{N(T_{min}, \Delta t_3)} \tag{7}$$

and is plotted in Figure 24 as a function of the ratio $\bar{R}_{t_I}$ of the mean running times $\bar{t}_I$

$$\bar{R}_{t_I} = \frac{\bar{t}_I(h;T_{max}, \Delta t_1)}{\bar{t}_I(h;T_{min}, \Delta t_3)} \tag{8}$$

where the $\bar{t}_I$'s represent the combined CPU and I/O values of the execution step, averaged over inclination*, for simultaneous calculations of electron and proton fluxes.

The graph indicates that on the average a decrease in points by a factor of 10 reduces computer time by about a factor of 2.4. The straight line is an attempt to eliminate the scatter in the data and linearize the R_p to $\bar{R}_{t_I}$ relationship, which can be expressed as

$$\bar{R}_{t_I} = 0.1R_p + 1.4 \tag{9}$$

*All times relate to an IBM 360/91 operating system.

Equation (9) should hold for other operating systems on computers with similar CPU and I/O algorithms, regardless of trajectory or models, as long as the orbital flux integration programs are similar in structure and complexity to the UNIFLUX system (see Appendix), used in the present calculations.

It should be pointed out, that statistically the R_p to $\overline{R}_{t_I}$ relationship is independent of altitude and inclination because as indicated above, the running times were first averaged over inclination at each altitude level, for the duration and stepsize of interest, and then the per altitude values were folded into the final curve. On the case by case basis, there are of course differences; for example, it was observed that at altitudes of $h \lesssim 16000$ km, polar and/or equatorial orbits required consistently less time than the other two intermediate inclinations; this apparent differentiation occurred at most durations and stepsizes. No explanation can readily be given for this peculiarity in timing, especially not in view of the fact that the total number of points treated per fixed h, T, and Δt were equal for all four inclinations. These variations may have to do with search and B/L-interpolation requirements in the environment models (TRARA1, TRARA2) and with the decay bypass feature in UNIFLUX.

Table 2 lists the total number of positions N (i.e. integration steps) that are contained in a trajectory of given duration and stepsize, for sets of values of T and Δt, where:

$$N = \frac{d \times T}{\Delta t} \qquad (10)$$

T is in hours, Δt in minutes, and the conversion constant d in minutes per hour.

Flux calculations are performed at these points. For any T then, the size of Δt determines the density with which the environment of a spacecraft is sampled.

An interesting picture emerges when the averaged-over-inclination running times of all investigated altitudes, durations, and stepsizes are coded by symbols according to number of points treated per run, and are then plotted as $\bar{t}_I(h;T, \Delta t)$ versus h; if in this process every $\bar{t}_I$ is also subscripted by its Δt, the plotted data is unambiguously identified as to its origin through equation (10). Figure 16 shows some of these inclination-averaged running times.

Two striking patterns are immediately apparent from Figure 16. First, that runs for high and very low altitudes require less time for the same number of points to be processed than runs at intermediate altitudes, with a maximum time consumption occurring at about 2000 kilometers; and second, that with increasing stepsize, progresssively more time was consumed by runs which in essence processed the same number of points.

No adequate explanation can be provided for the differentiation of the running times over h; maybe the trajectories at lower and higher altitudes require on the average fewer actual flux calculations because larger segments of their orbits lie outside the trapping regions of the models. The larger running times mentioned in the second observation can be attributed, partially at least, to the skipping mechanism in UNIFLUX, which is activated whenever the inputted stepsize is greater than an integer multiple of the constant orbit-tape time increment. Since all trajectories used in this study were generated with Δt=1 minute, this process may account for some of the additional time expended with larger Δt's.

If all trajectories of equal N value are grouped together and their running times t are averaged over altitude, inclination, duration, and stepsize, then the maximum variation from the mean, observed in the group, is less than 27%; it occurs only in large groups with 16 - 36 members and there only once, in one member. The average variation of the combined CPU-I/O time for all other members and groups is less than 10%. The mean running time for each group is plotted in Figure 17, which gives a good measure of program efficiency and optimization potential. Also plotted are the mean running times per point of the larger groups. The solid and dashed curves approximate a best fit to the means.

The non-linearity of the mean running times may be partially due to an initial element of time required by the computer to activate functions, to set up storage, to allocate core, to clear registers, etc. For extensive runs with a large number of positions, this initial time expenditure is then distributed over many points, thus minimizing the "penalty" per point, whereas for short runs with a small number of points, each point is charged with a correspondingly larger amount of initialization time.

Similar conditions should affect orbital flux integration runs on any computer. Of course, a difference in these conditions may alter the shape, slope, or amplitude of the curves in Figure 17.

In conclusion, it was determined that a perfectly reliable and useful orbital flux integration, if performed with the proposed optimal (for the investigated ranges of T and Δt) values of duration and stepsize, would on the average require only from about .1 to .3

minutes of computer CPU-I/O time, depending on the altitude. All the test calculations were performed on an IBM 360/91 multiprocessor system with the new UNIFLUX program (Stassinopoulos and Gregory, 1974). It is to be expected that other codes on other machines may produce different absolute running times or flux results. However, the respective optimization effects should be analogous and the relative R_P and $\overline{R}_{tI}$ ratios should be similar for equivalent runs.

SUMMARY

It has been shown, that within the limit of accuracy and ranges of parameters, a duration of 24 hours is sufficient to insure an adequate sampling of spacecraft environments in circular subsynchronous orbits, and that an increase in T, while raising the number of points to be treated and expending more computer time, does not meaningfully improve the integration results.

It has also been established that stepsize in general is a function of altitude alone and does not depend on inclination or duration. A functional relationship was developed to yield an optimal Δt for any given h between 200 and 32000 kilometers.

Acknowledgements

The author wishes to thank Dr. James I. Vette for many helpful suggestions and for reviewing the manuscript. Thanks are also due to Mr. Joel Hebert for his very valuable programming assistance.

References

Stassinopoulos, E. G., and C. Z. Gregory, "UNIFLUX: A Unified Orbital Flux Integration and Analysis System"; to be published in 1975.

Singley, G. W., and J. I. Vette, "A Model Environment for Outer Zone Electrons,", NSSDC 72-13, National Space Science Data Center, Greenbelt, Maryland, July, 1972.

Teague, M. J., and J. I. Vette, "The Inner Zone Electron Model AE-5", NSSDC 72-10, National Space Science Data Center, Greenbelt, Maryland, September, 1972.

Lavine, J. P., and J. I. Vette, Models of the Trapped Radiation Environment, Volume V: Inner Belt Protons, NASA SP-3024, 1969.

McIlwain, C. E., "Coordinates for Mapping the Distribution of Magnetically Trapped Particles", J. Geophysical Research, 66, 3681, 1961.

APPENDIX

UNIFLUX: A Unified Orbital Flux Integration and Analysis System

The system, developed by E. G. Stassinopoulos & C. Z. Gregory (1974) at Goddard Space Flight Center, combines into one compact program package several previously separate or independent functions and operations. It affords the user great flexibility as to selections of particle species, of threshold energies, of types of orbits, etc., and it permits the treatment of special cases, previously excluded from consideration. It offers more choices as to type, form, and format of output; it has greatly expanded capabilities for the presentation of results, providing additional information obtained through programmed data analysis. Most importantly, however, the system requires less core storage and is significantly faster than comparable computer programs presently in use.

UNIFLUX incorporates the currently valid proton and electron environment models in matrix storage form (the new Kluge-Lenhart mode). It is capable of decaying artificial Starfish electrons, still contained in the latest solar-max electron models, down to approximately natural background levels. Included in the program is also a solar proton model and a method to calculate the exposure of a spacecraft to energetic solar protons for energies from 10 to 100 Mev.

Special Features of UNIFLUX are:

a) unrestricted multiple orbit capability (in one execution step)

b) liberalized plot selection (increased freedom of choice)

c) optional accumulative B/L-bin account (output can be suppressed)

d) selective integration stepsize (independent of trajectory time-increment)

e) analytical differentiation of orbit integrated spectra

f) multiple output-table production capability (to print set of tables any specified number of times)

g) simultaneous (combined) processing of all electron and proton models during a single execution and I/O step (one run for all models, all species).

The program is available upon request from the National Space Science Data Center, Code 601, Goddard Space Flight Center, Greenbelt, Maryland, 20771.

TABLE 1

Evaluation of Duration and Stepsize Requirements of Orbital Flux Integrations

Orbit Parameters and Integrations Variables

h Altitude (km)	Period (hrs)	P/τ Orbital Precession (degr/hr)	Daily Advance (degr/day)	T Tested Durations (hrs)	Δt Tested Integration Stepsizes (mins)
400	1.5427	23.14	6.64	24	1,2,3
1000	1.752	26.28	4.52	24	1,2,3
2200	2.196	32.94	1.07	24,48	1,2,3
4000	2.923	43.85	11.85	24,48,72	1,3,5
16000	9.254	138.81	6.10	24,48,72,96	2,4,6
30000	19.999	299.99	60.01	24,72,96	3,6,9

Note: At all specified altitudes, four inclinations were considered in the tests:

$i = 0^{\circ}, 30^{\circ}, 60^{\circ}, 90^{\circ}$.

TABLE 2

Number of samplings in trajectories with duration T

and Stepsize Δt

T \ Δt	1	2	3	4	5	6	9	10
24	1440	720	480	360	288	240	160	144
48	2880	1440	960	720	576	480	320	288
72	4320	2160	1440	1080	864	720	480	432
96	5760	2880	1920	1440	1152	960	640	576

Note: Values underlined were used in one or more of the calculations.

TABLE 3

Orbital Flux Integration Parameters:

Stepsizes and Durations per Altitude

(Circular Orbits)

h (km)	i (degr)	T (hrs)	Δt (min)
400	0, 30, 60, 90	24	(1) 2 (3)
1000	0, 30, 60, 90	24	(1) 2 (3)
2200	0, 30, 60, 90	24	1 2 (3)
		48	(1) 2 3
4000	0, 30, 60, 90	24	1 3 (5)
		48	1 3 5
		72	(1) 3 5
16000	0, 30, 60, 90	24	2 4 (6)
		48	2 4 6
		72	2 4 6
		96	(2) 4 6
30000	0, 30, 60, 90	24	3 6 (9)
		72	3 6 9
		96	(3) 6 9

(O): circles, at the corresponding duration levels, indicate the stepsizes with which the data, used in the transverse comparison, were obtained.

Table 4

Duration Dependence of Simple Deviations[+]

Case showing no improvement with increase of duration

h(km)	Stepsize(mins) Δt_1	Stepsize(mins) Δt_3	Species	i(degr)	Simple Deviations |D| % for T(hrs) 24	48	72	96
2200	1	3	e	30	0	.84		
				60	.09	.32		
				90	.05	.27		
			p	0	0	.10		
4000	1	5	e	60	.14	.19	*	
				90	*	.06	.17	
			p	60	*	.03	.10	
				90	*	0	.08	
16000	2	6	e	0	← no change →			
				30	.02	.02	0	0
				90	*	.05	.05	.05
			p	0	*	0	.07	.07
				30	.07	.07	.07	*
30000	3	9	e	0	.18		.19	*
				90	*		.24	.25

* not applicable for this comparison

+ $$D = \frac{F(T;\Delta t_1) - F(T;\Delta t_3)}{F(T;\Delta t_1)}$$

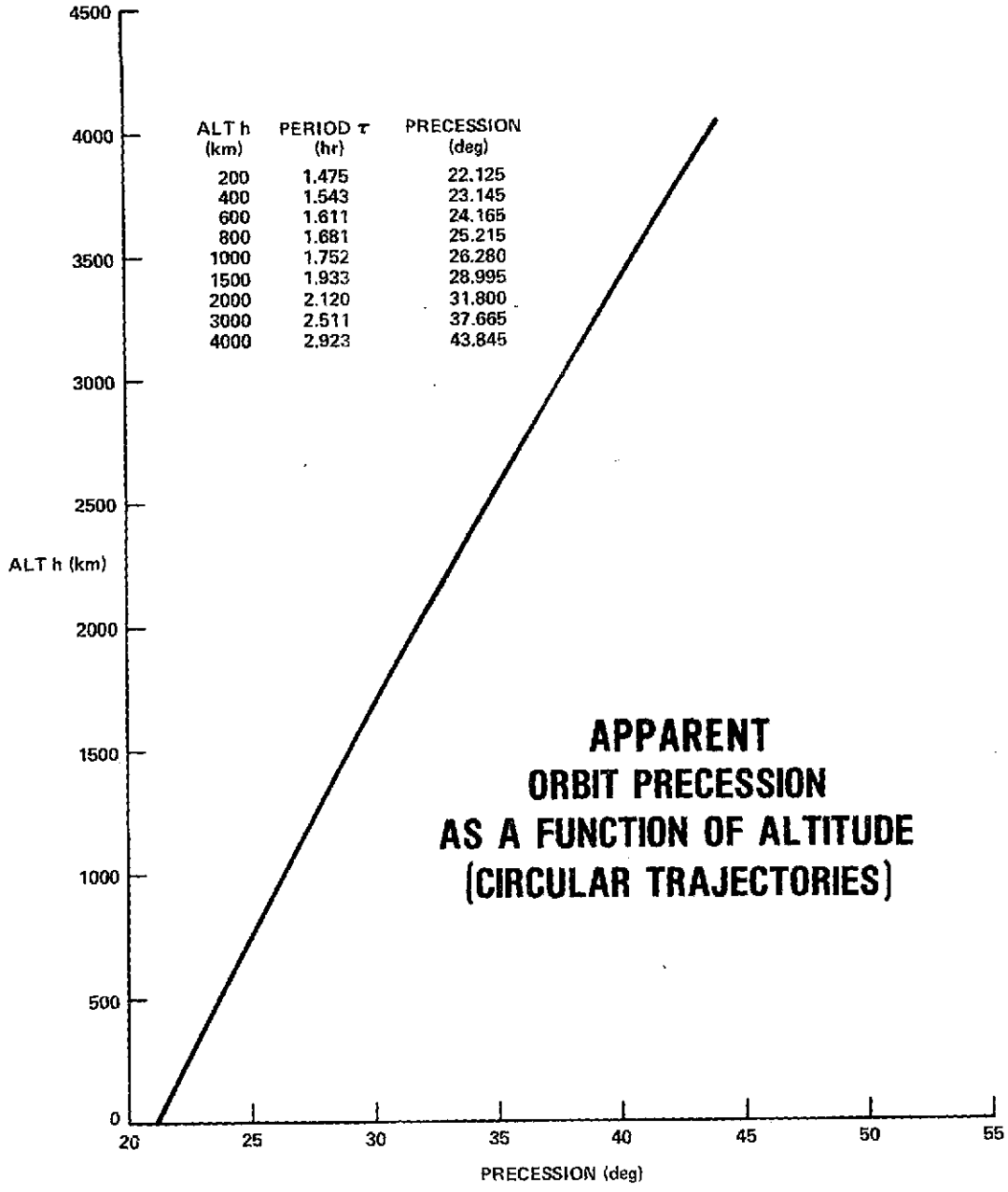
ALT h (km)
PERIOD τ (hr)
PRECESSION (deg)
200 1.475 22.125
400 1.543 23.145
600 1.611 24.165
800 1.681 25.215
1000 1.752 26.280
1500 1.933 28.995
2000 2.120 31.800
3000 2.511 37.665
4000 2.923 43.845
APPARENT
ORBIT PRECESSION
AS A FUNCTION OF ALTITUDE
(CIRCULAR TRAJECTORIES)
ALT h (km)
PRECESSION (deg)
4500
4000
3500
3000
2500
2000
1500
1000
500
0
20
25
30
35
40
45
50
55

Figure 1

ELECTRON FLUX CONTOURS–E>0.5 MeV

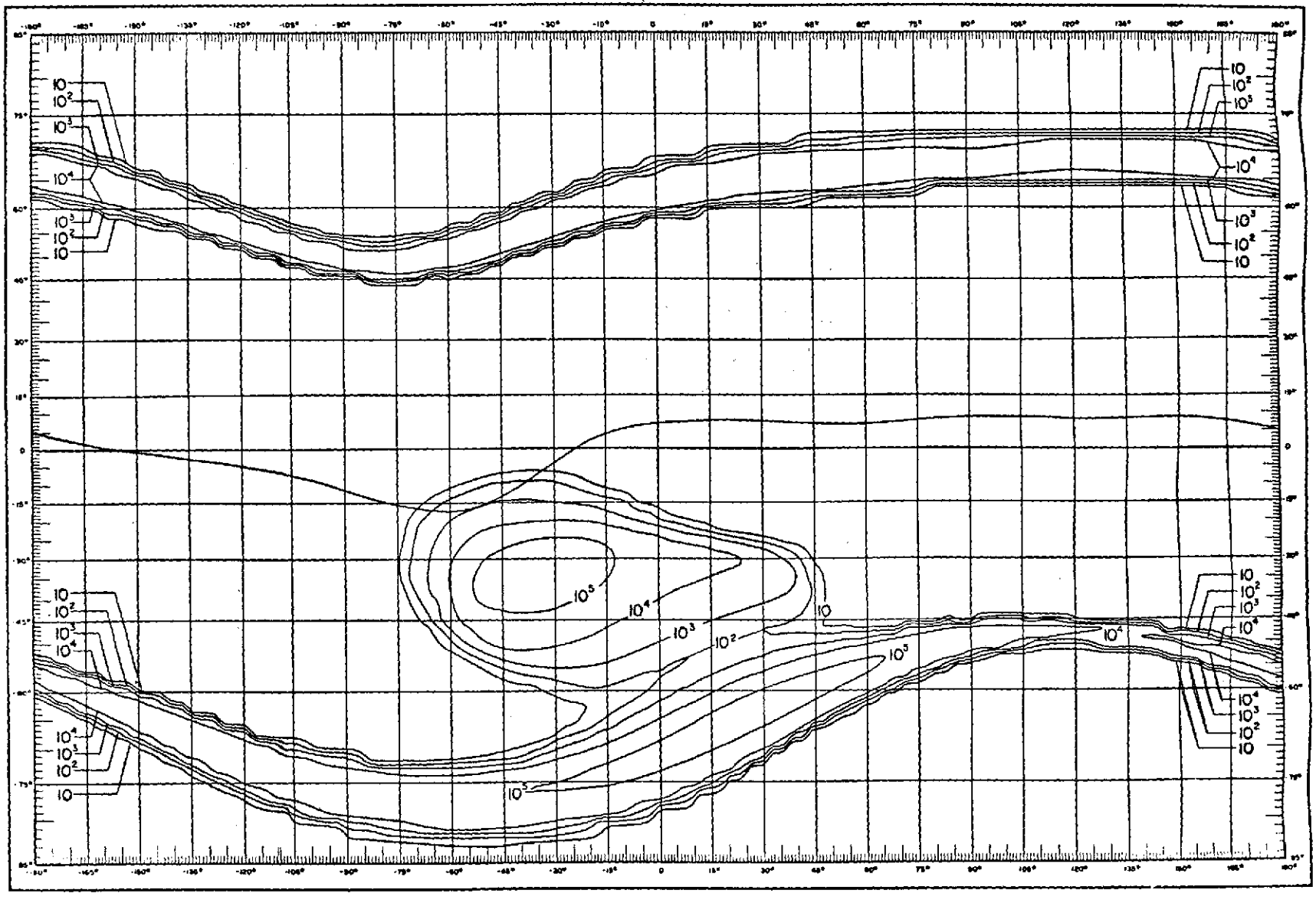

ALTITUDE = 300 KM

Figure 2

ELECTRON FLUX CONTOURS—E > 0.5 MeV

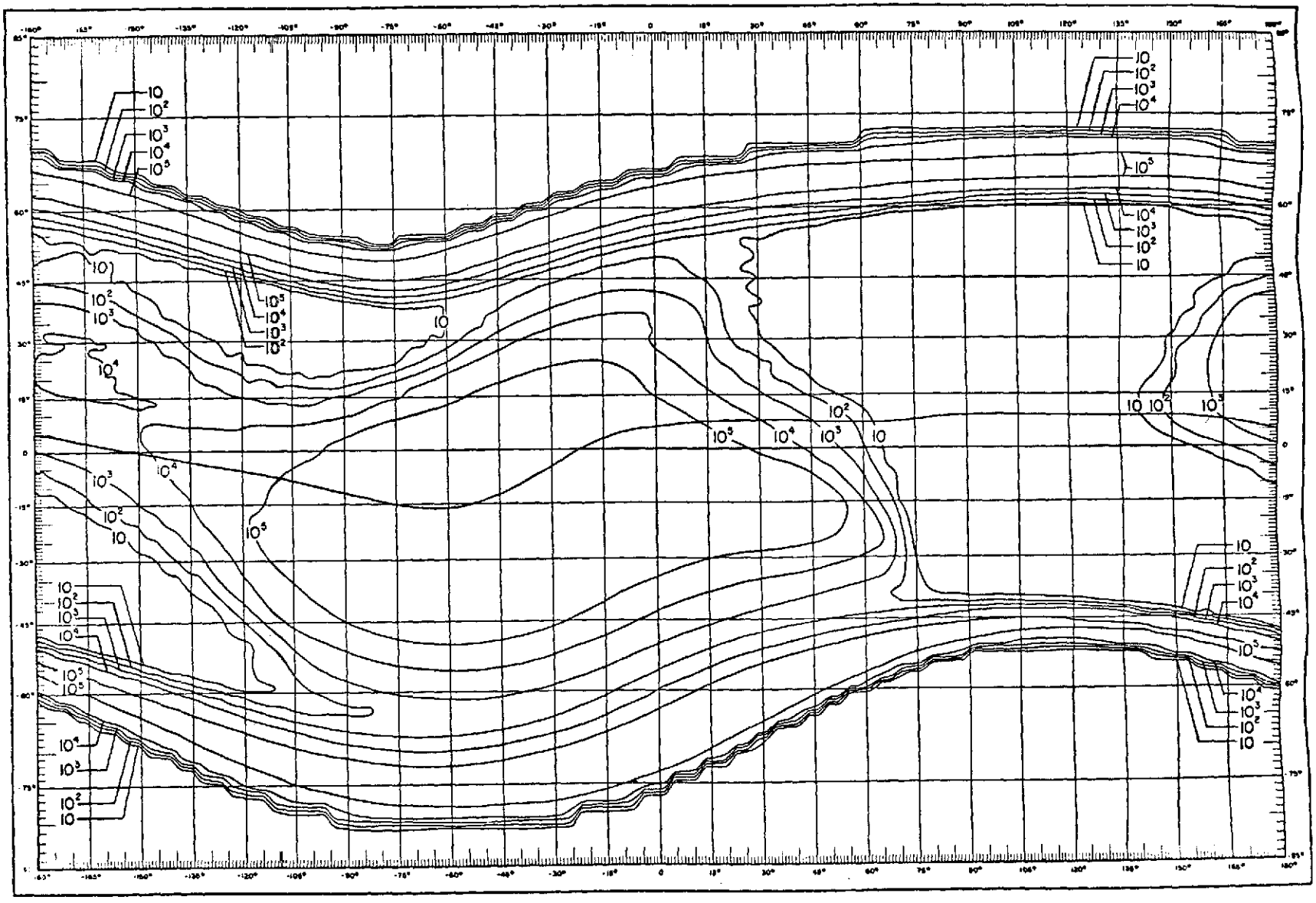

ALTITUDE = 1000 KM

Figure 3

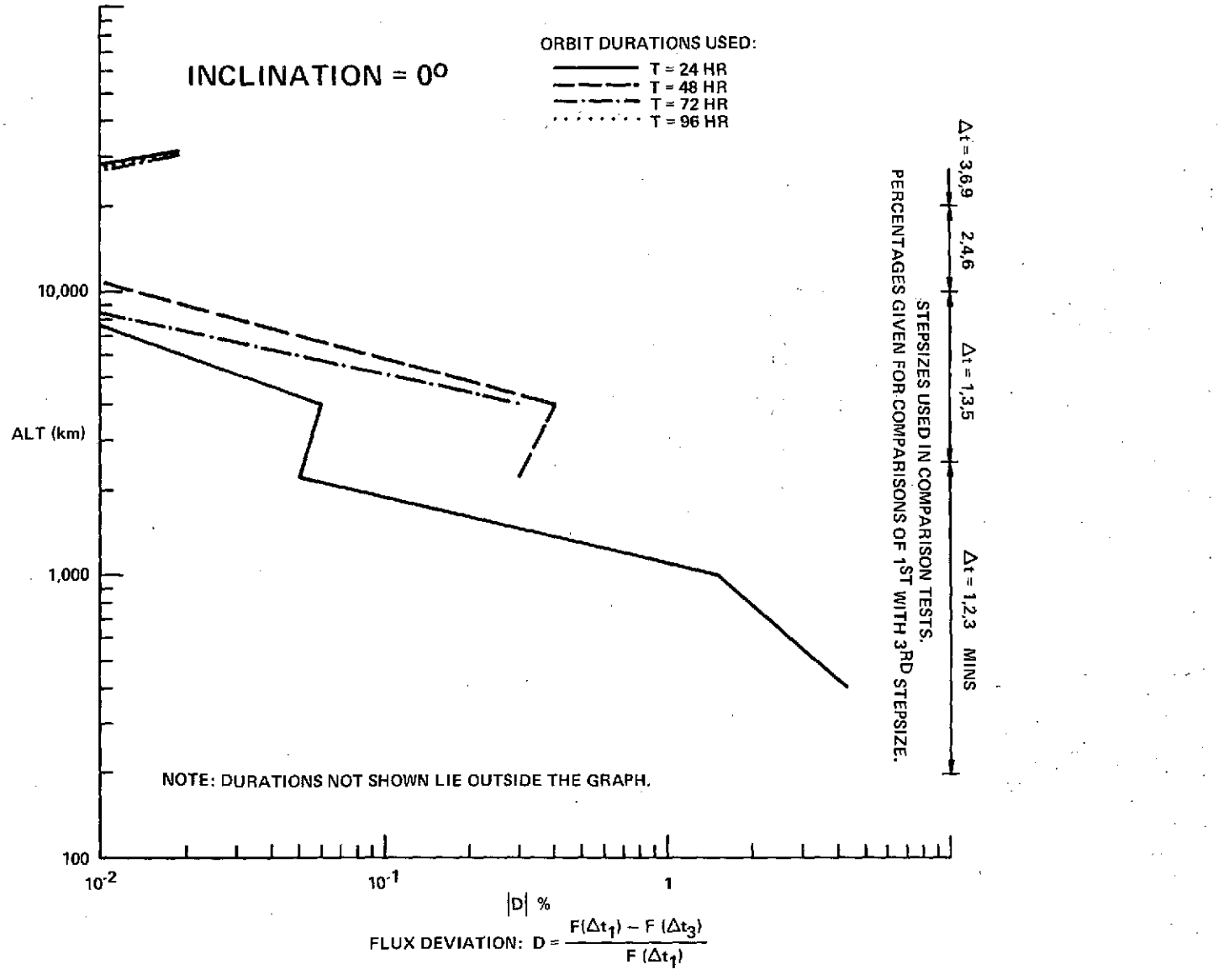
ELECTRONS (E > 0.5 MeV)
INCLINATION = 0°
ORBIT DURATIONS USED:
T = 24 HR
T = 48 HR
T = 72 HR
T = 96 HR
ALT (km)
10,000
1,000
100
NOTE: DURATIONS NOT SHOWN LIE OUTSIDE THE GRAPH.
10^{-2}
10^{-1}
1
|D| %
FLUX DEVIATION: $D = \frac{F(\Delta t_1) - F(\Delta t_3)}{F(\Delta t_1)}$
PERCENTAGES GIVEN FOR COMPARISONS OF 1ST WITH 3RD STEPSIZE.
STEPSIZES USED IN COMPARISON TESTS.
Δt = 3,6,9
2,4,6
Δt = 1,3,5
Δt = 1,2,3 MINS

Figure 4a

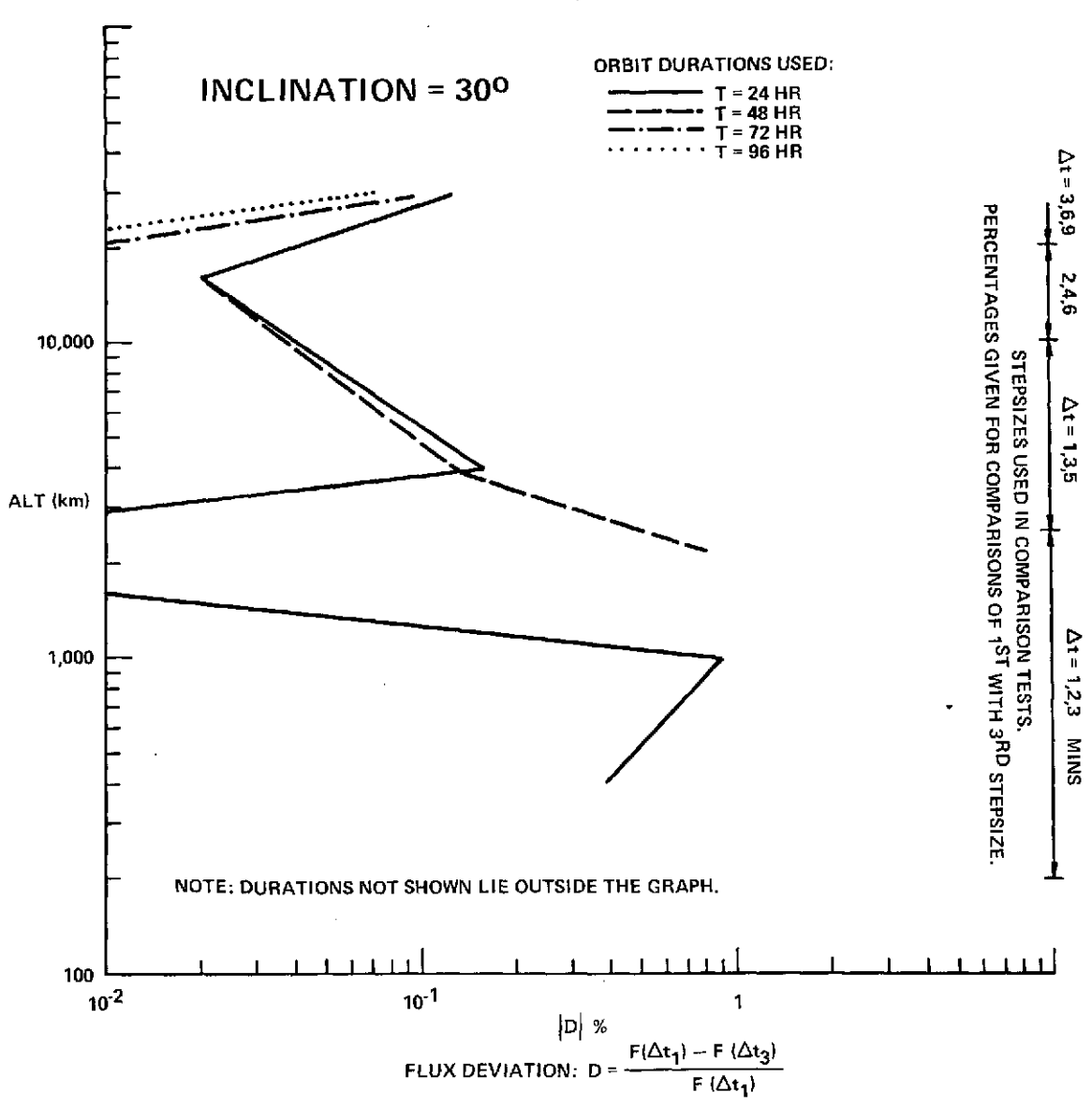
ELECTRONS (E > 0.5 MeV)
INCLINATION = 30°
ORBIT DURATIONS USED:
T = 24 HR
T = 48 HR
T = 72 HR
T = 96 HR
ALT (km)
10,000
1,000
100
10^{-2}
10^{-1}
1
|D| %
NOTE: DURATIONS NOT SHOWN LIE OUTSIDE THE GRAPH.
FLUX DEVIATION: $D = \frac{F(\Delta t_1) - F(\Delta t_3)}{F(\Delta t_1)}$
PERCENTAGES GIVEN FOR COMPARISONS OF 1ST WITH 3RD STEPSIZE.
STEPSIZES USED IN COMPARISON TESTS.
Δt = 3,6,9
2,4,6
Δt = 1,3,5
Δt = 1,2,3 MINS

Figure 4b

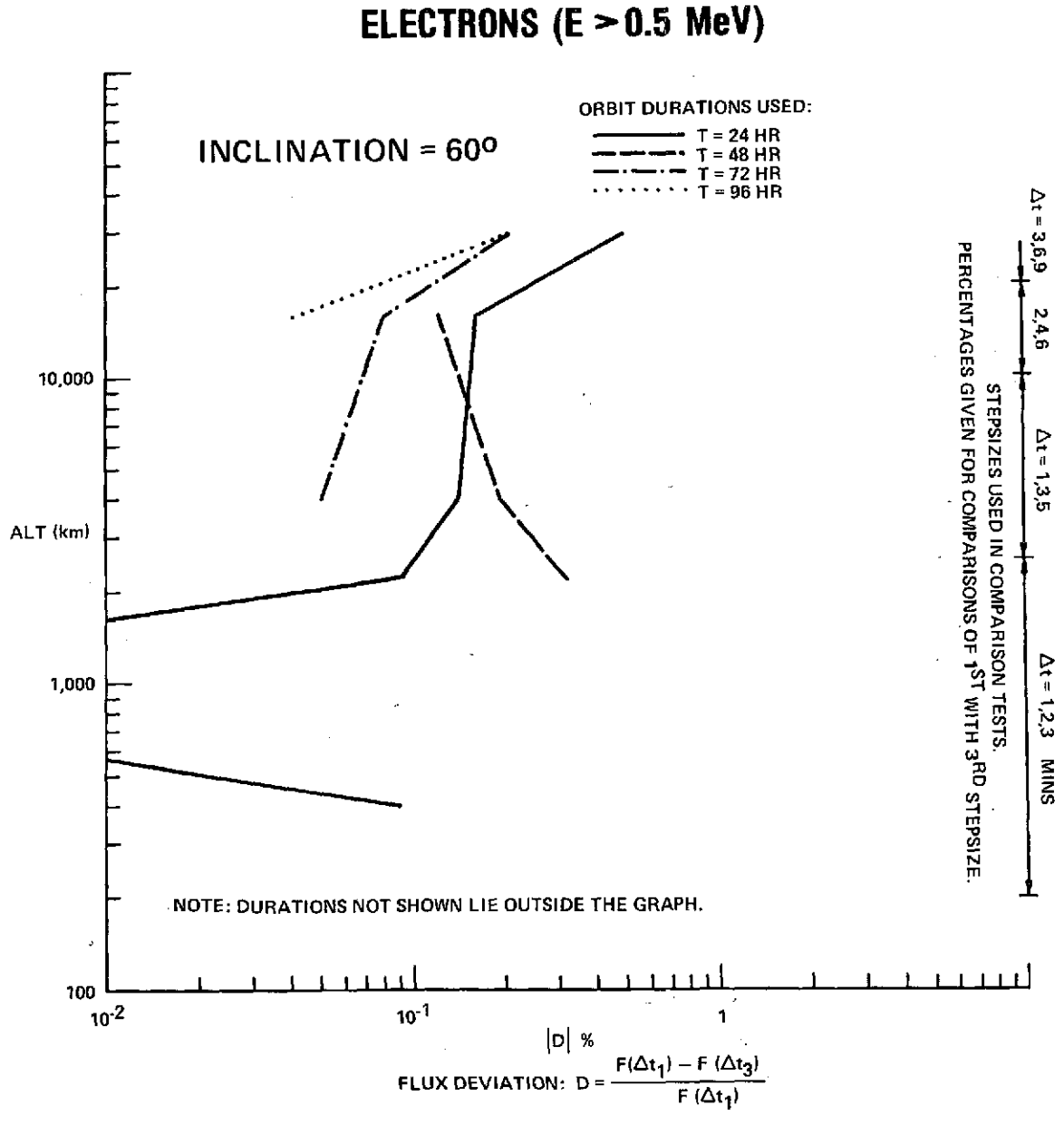
ELECTRONS (E > 0.5 MeV)
INCLINATION = 60°
ORBIT DURATIONS USED:
T = 24 HR
T = 48 HR
T = 72 HR
T = 96 HR
ALT (km)
10,000
1,000
100
NOTE: DURATIONS NOT SHOWN LIE OUTSIDE THE GRAPH.
10^{-2}
10^{-1}
1
|D| %
FLUX DEVIATION: $D = \frac{F(\Delta t_1) - F(\Delta t_3)}{F(\Delta t_1)}$
PERCENTAGES GIVEN FOR COMPARISONS OF 1ST WITH 3RD STEPSIZE.
STEPSIZES USED IN COMPARISON TESTS.
Δt = 3,6,9
2,4,6
Δt = 1,3,5
Δt = 1,2,3 MINS

Figure 4c

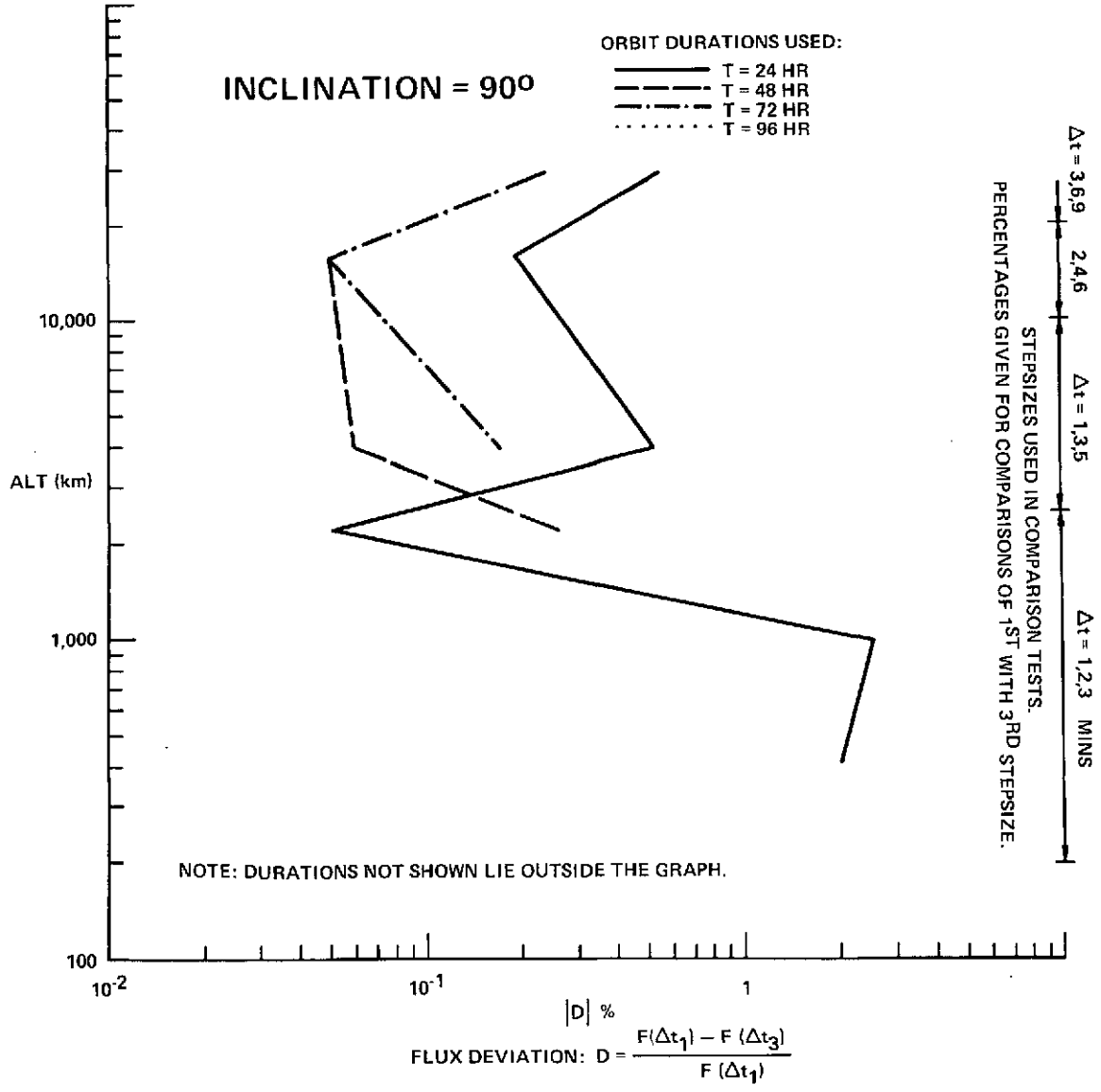
ELECTRONS (E > 0.5 MeV)
INCLINATION = 90°
ORBIT DURATIONS USED:
T = 24 HR
T = 48 HR
T = 72 HR
T = 96 HR
ALT (km)
10,000
1,000
100
10^{-2}
10^{-1}
1
|D| %
FLUX DEVIATION: $D = \frac{F(\Delta t_1) - F(\Delta t_3)}{F(\Delta t_1)}$
NOTE: DURATIONS NOT SHOWN LIE OUTSIDE THE GRAPH.
PERCENTAGES GIVEN FOR COMPARISONS OF 1ST WITH 3RD STEPSIZE.
STEPSIZES USED IN COMPARISON TESTS.
Δt = 3,6,9
2,4,6
Δt = 1,3,5
Δt = 1,2,3 MINS

Figure 4d

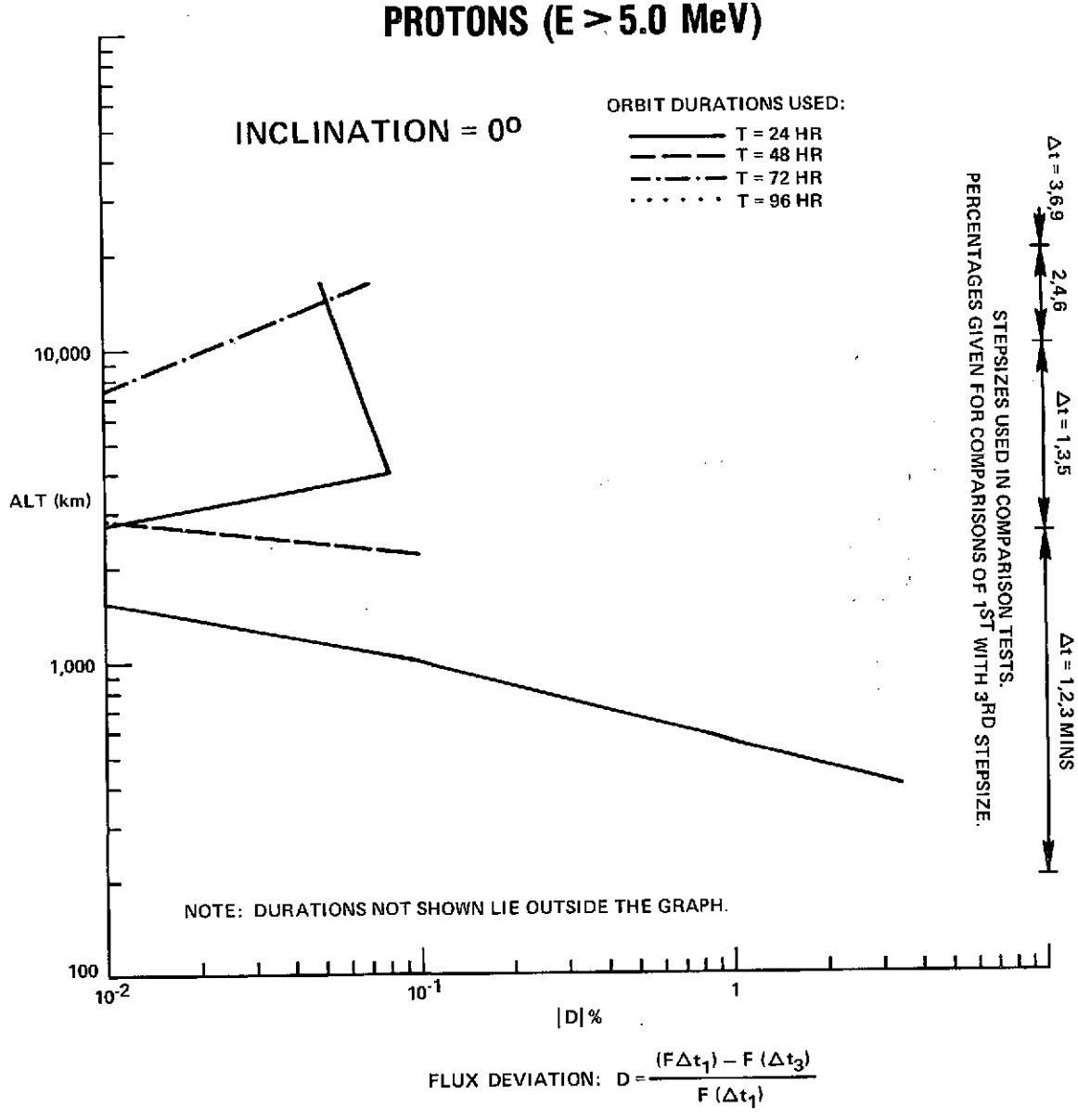
PROTONS (E > 5.0 MeV)
INCLINATION = 0°
ORBIT DURATIONS USED:
T = 24 HR
T = 48 HR
T = 72 HR
T = 96 HR
Δt = 3,6,9
2,4,6
Δt = 1,3,5
Δt = 1,2,3 MINS
STEPSIZES USED IN COMPARISON TESTS.
PERCENTAGES GIVEN FOR COMPARISONS OF 1ST WITH 3RD STEPSIZE.
10,000
ALT (km)
1,000
100
NOTE: DURATIONS NOT SHOWN LIE OUTSIDE THE GRAPH.
10-2
10-1
1
|D|%
FLUX DEVIATION: D = (FΔt1) – F (Δt3) / F (Δt1)

Figure 5a

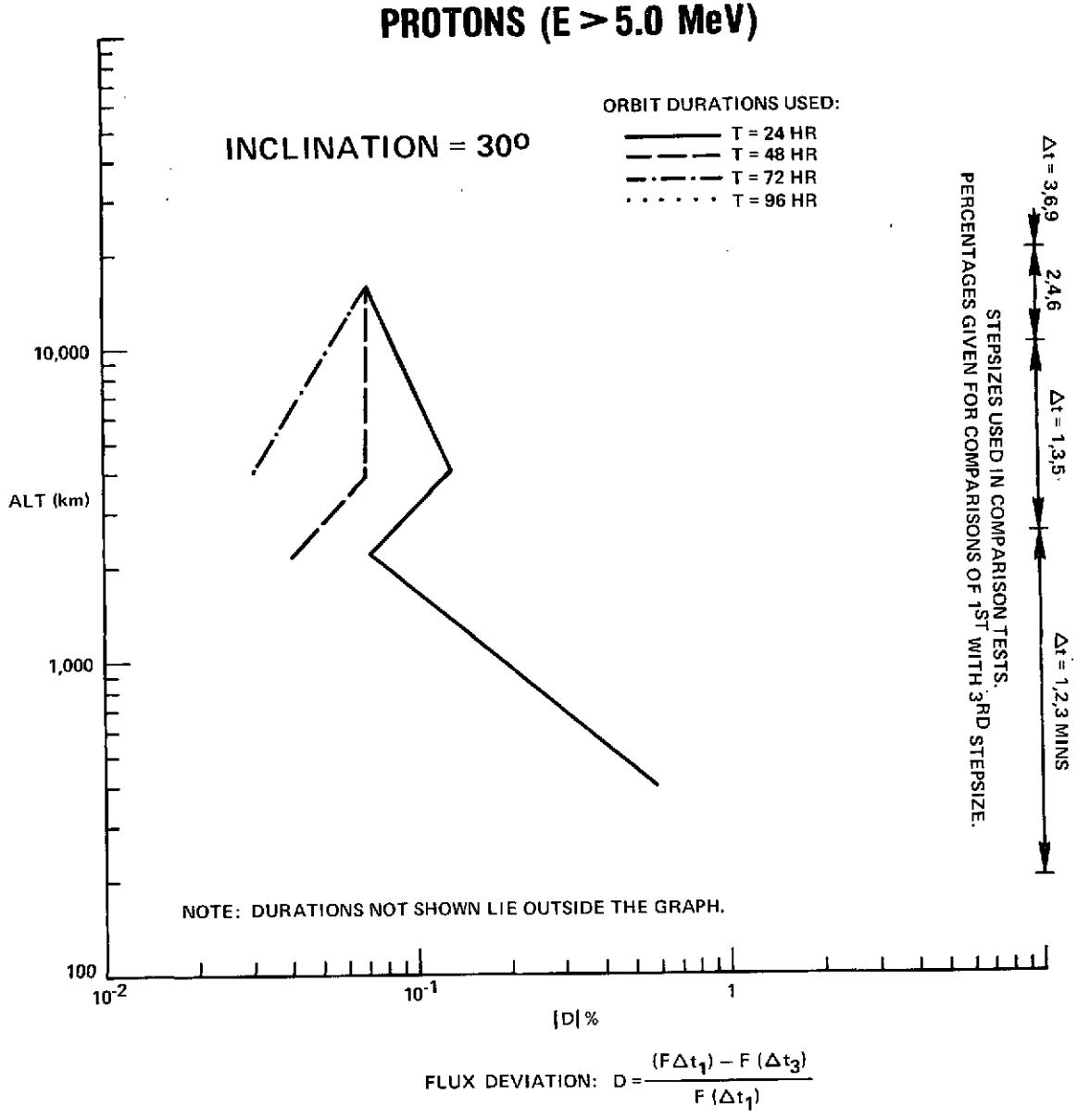
PROTONS (E > 5.0 MeV)
INCLINATION = 30°
ORBIT DURATIONS USED:
T = 24 HR
T = 48 HR
T = 72 HR
T = 96 HR
STEPSIZES USED IN COMPARISON TESTS.
PERCENTAGES GIVEN FOR COMPARISONS OF 1ST WITH 3RD STEPSIZE.
Δt = 3,6,9
2,4,6
Δt = 1,3,5
Δt = 1,2,3 MINS
ALT (km)
10,000
1,000
100
NOTE: DURATIONS NOT SHOWN LIE OUTSIDE THE GRAPH.
10-2
10-1
1
|D| %
FLUX DEVIATION: D = (FΔt1) – F (Δt3) / F (Δt1)

Figure 5b

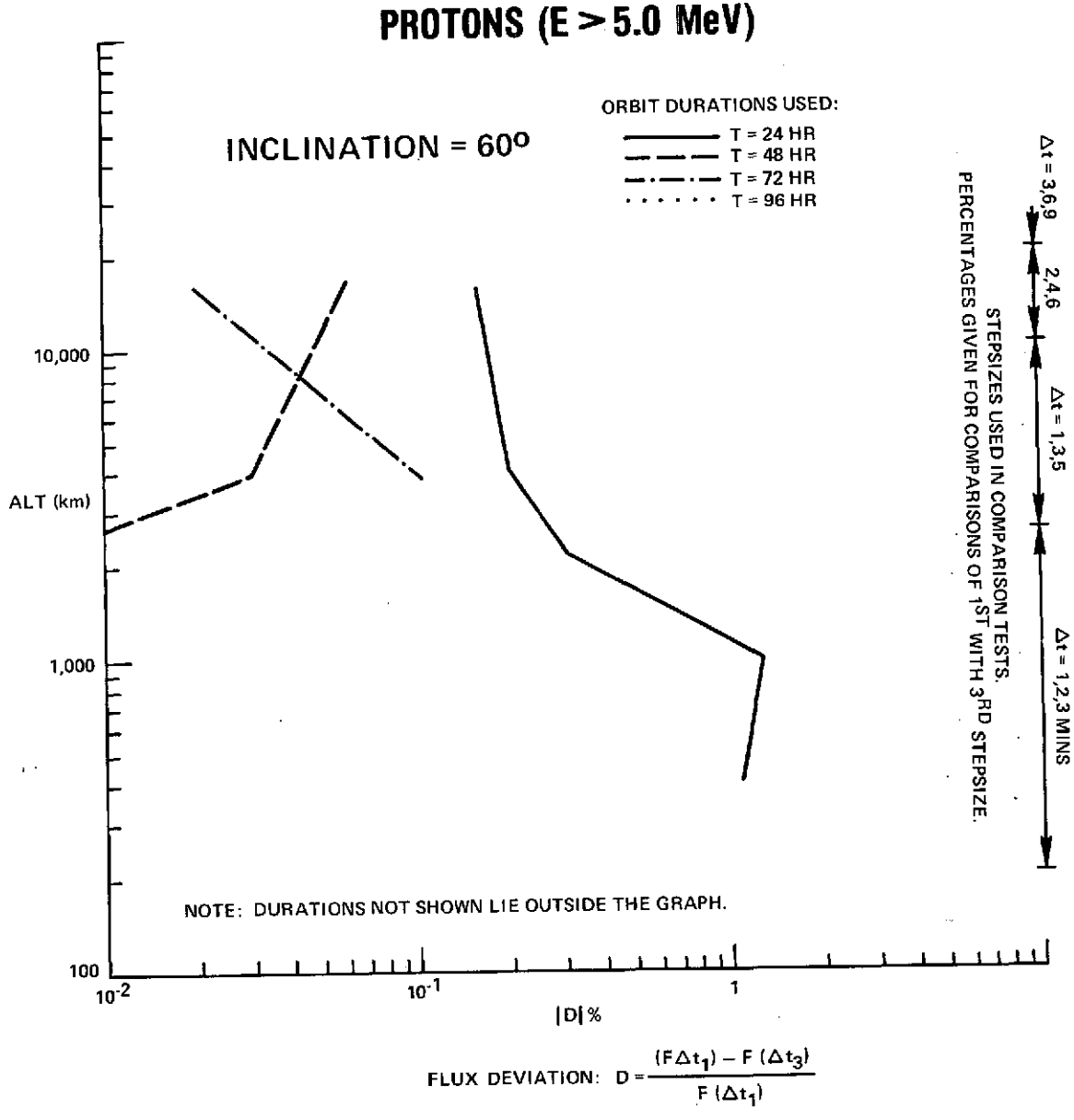
PROTONS (E > 5.0 MeV)
INCLINATION = 60°
ORBIT DURATIONS USED:
T = 24 HR
T = 48 HR
T = 72 HR
T = 96 HR
ALT (km)
10,000
1,000
100
10^{-2}
10^{-1}
1
|D|%
NOTE: DURATIONS NOT SHOWN LIE OUTSIDE THE GRAPH.
STEPSIZES USED IN COMPARISON TESTS.
PERCENTAGES GIVEN FOR COMPARISONS OF 1ST WITH 3RD STEPSIZE.
Δt = 3,6,9
2,4,6
Δt = 1,3,5
Δt = 1,2,3 MINS
FLUX DEVIATION: $D = \frac{(F\Delta t_1) - F(\Delta t_3)}{F(\Delta t_1)}$

Figure 5c

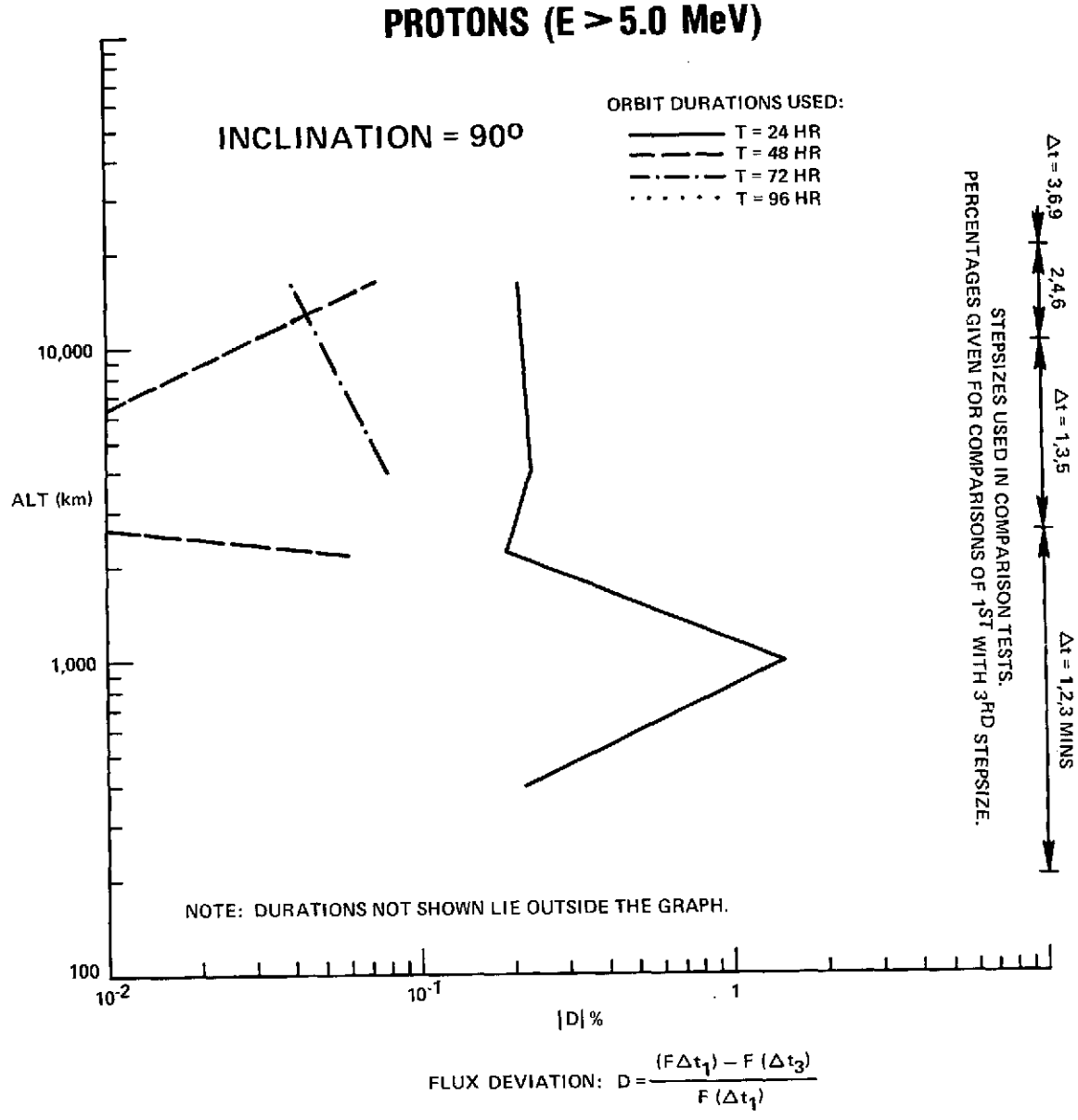
PROTONS (E > 5.0 MeV)
INCLINATION = 90°
ORBIT DURATIONS USED:
T = 24 HR
T = 48 HR
T = 72 HR
T = 96 HR
Δt = 3,6,9
2,4,6
Δt = 1,3,5
Δt = 1,2,3 MINS
STEPSIZES USED IN COMPARISON TESTS.
PERCENTAGES GIVEN FOR COMPARISONS OF 1ST WITH 3RD STEPSIZE.
ALT (km)
10,000
1,000
100
NOTE: DURATIONS NOT SHOWN LIE OUTSIDE THE GRAPH.
10^-2
10^-1
1
|D| %
FLUX DEVIATION: D = (F Δt1) − F (Δt3) / F (Δt1)

Figure 5d

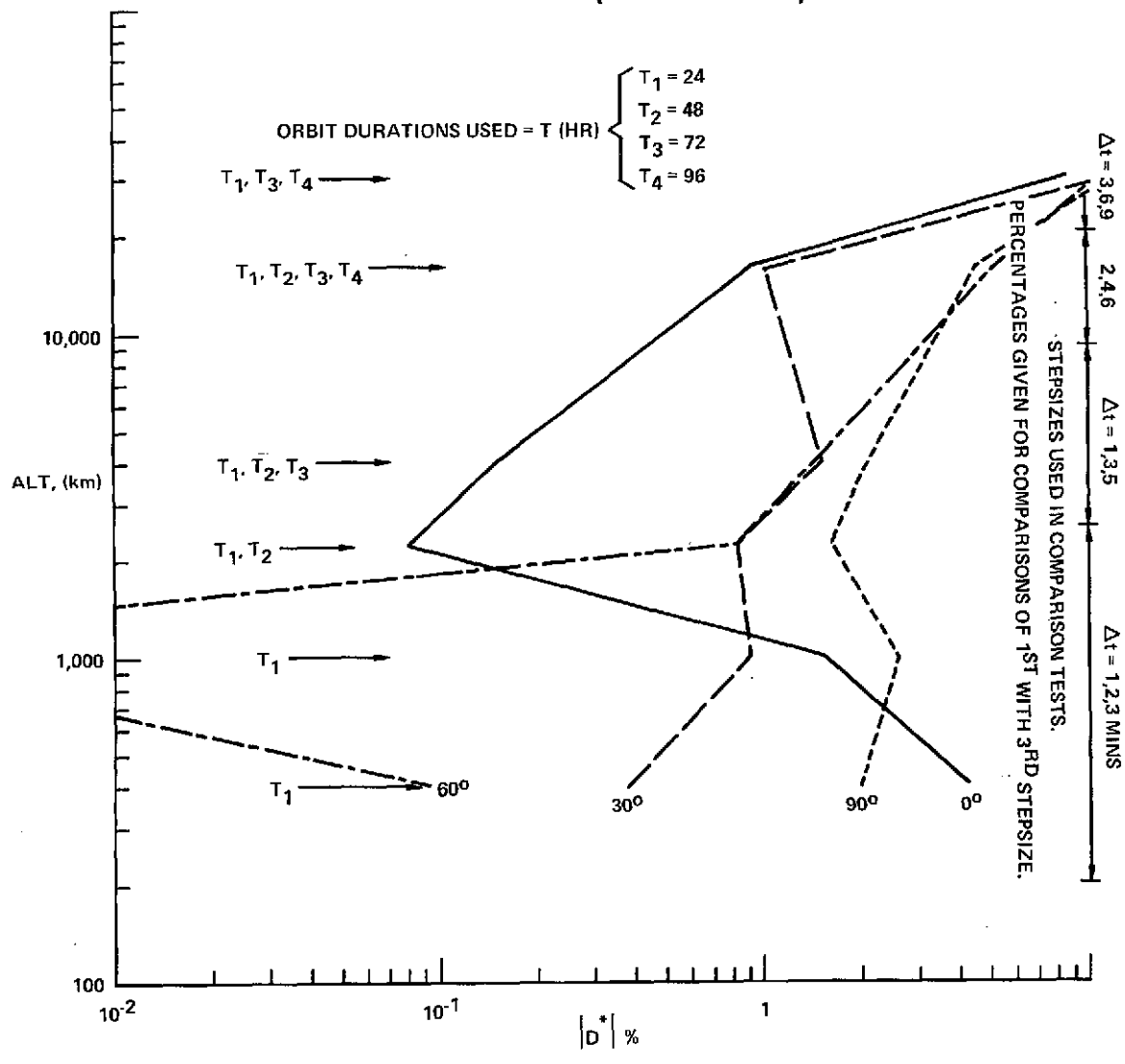

TRANSVERSE FLUX DEVIATION:

$$D^* = \frac{F(T_{max},\Delta t_1) - F(T_{min},\Delta t_3)}{F(T_{max},\Delta t_1)}$$

Figure 6

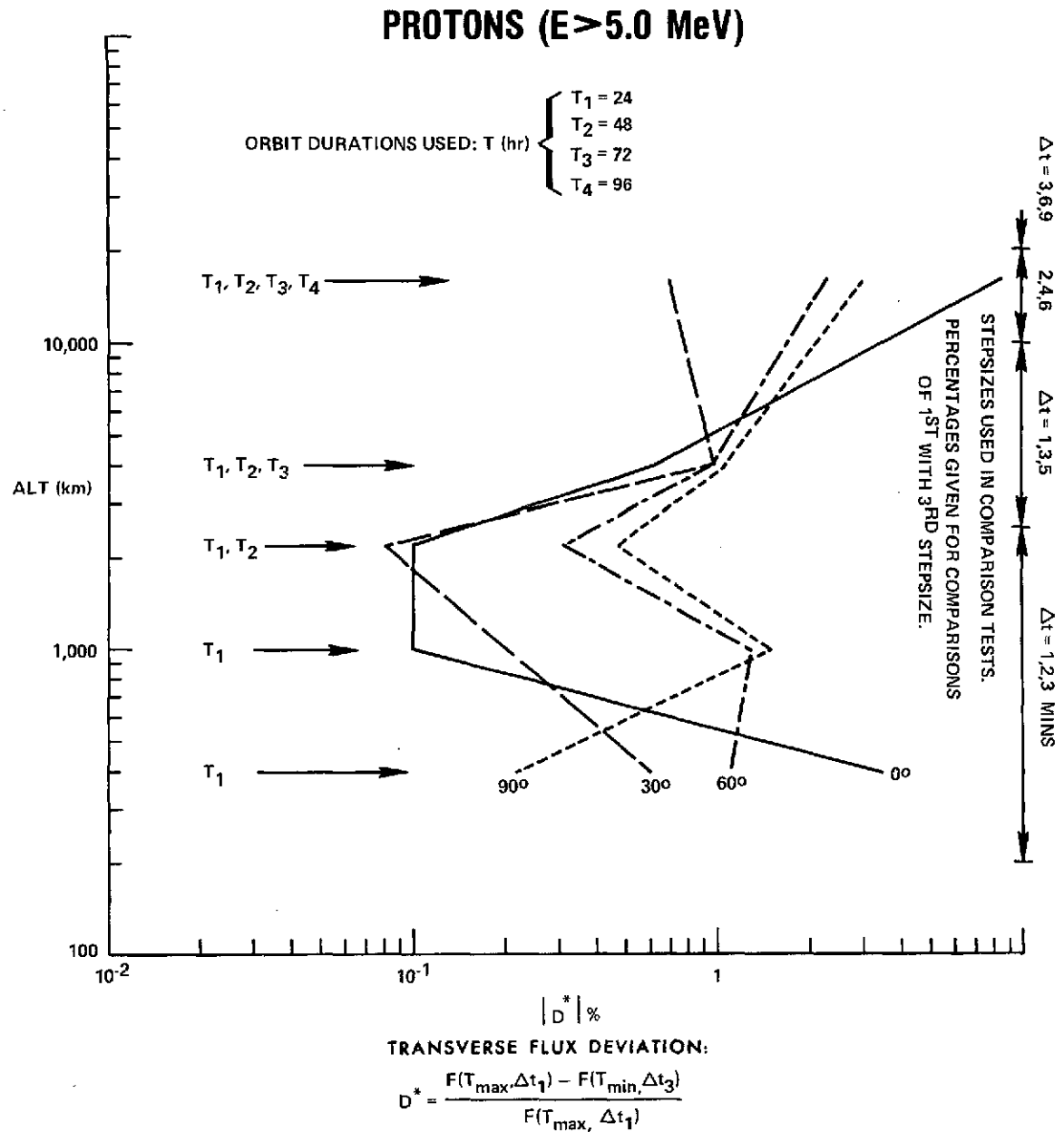
PROTONS (E>5.0 MeV)
ORBIT DURATIONS USED: T (hr)
T1 = 24
T2 = 48
T3 = 72
T4 = 96
T1, T2, T3, T4
T1, T2, T3
T1, T2
T1
T1
10,000
1,000
100
ALT (km)
90°
30°
60°
0°
Δt = 3,6,9
2,4,6
Δt = 1,3,5
Δt = 1,2,3 MINS
STEPSIZES USED IN COMPARISON TESTS.
PERCENTAGES GIVEN FOR COMPARISONS
OF 1ST WITH 3RD STEPSIZE.
10-2
10-1
1
|D*| %
TRANSVERSE FLUX DEVIATION:
D* = F(Tmax,Δt1) − F(Tmin,Δt3) / F(Tmax, Δt1)

Figure 7

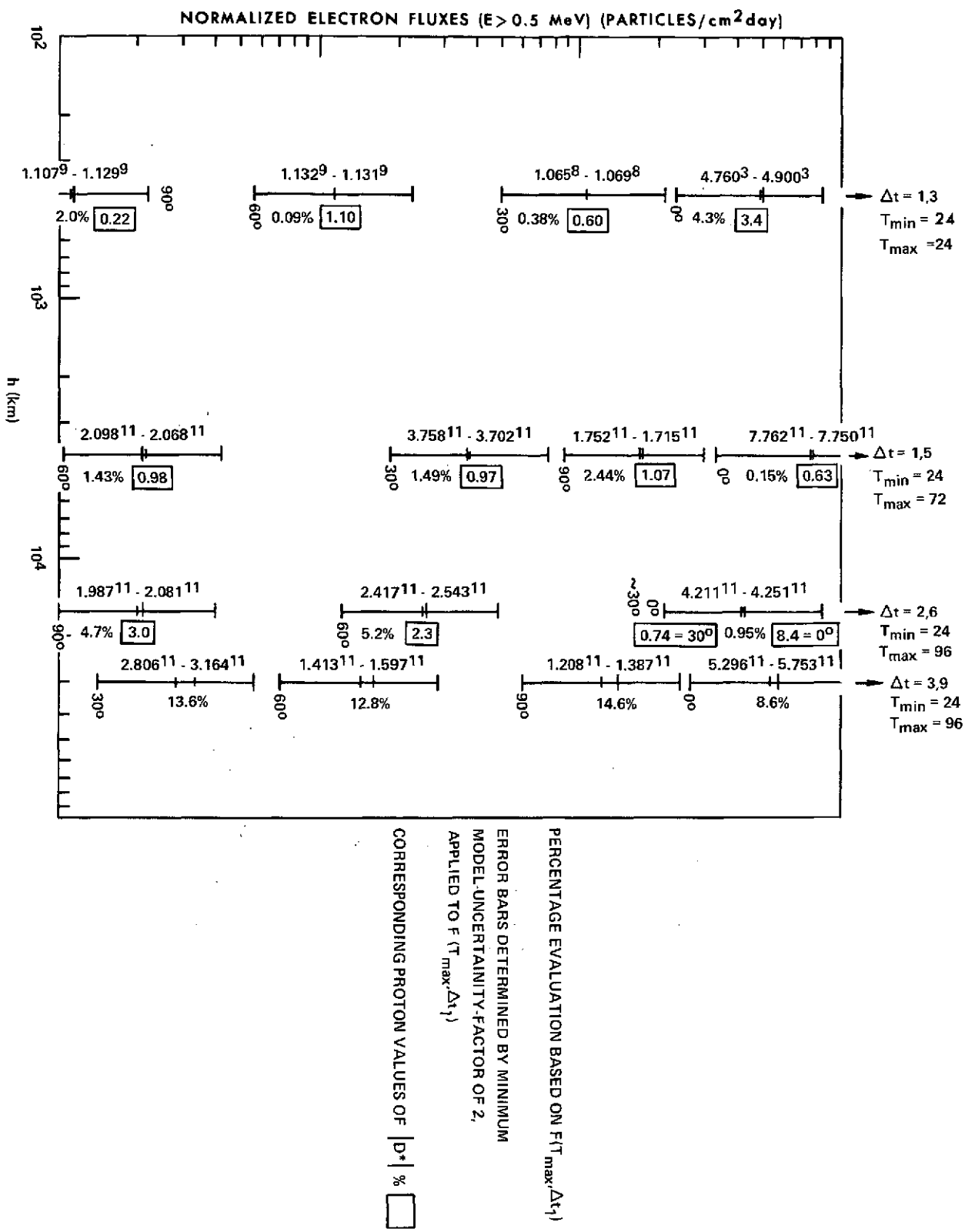
NORMALIZED ELECTRON FLUXES (E > 0.5 MeV) (PARTICLES/cm²day)
h (km)
10²
10³
10⁴
1.107⁹ - 1.129⁹
90°
2.0% 0.22
1.132⁹ - 1.131⁹
60°
0.09% 1.10
1.065⁸ - 1.069⁸
30°
0.38% 0.60
4.760³ - 4.900³
0°
4.3% 3.4
Δt = 1,3
T_min = 24
T_max = 24
2.098¹¹ - 2.068¹¹
60°
1.43% 0.98
3.758¹¹ - 3.702¹¹
30°
1.49% 0.97
1.752¹¹ - 1.715¹¹
90°
2.44% 1.07
7.762¹¹ - 7.750¹¹
0°
0.15% 0.63
Δt = 1,5
T_min = 24
T_max = 72
1.987¹¹ - 2.081¹¹
90°
4.7% 3.0
2.417¹¹ - 2.543¹¹
60°
5.2% 2.3
~30°
4.211¹¹ - 4.251¹¹
0°
0.74 = 30°
0.95% 8.4 = 0°
Δt = 2,6
T_min = 24
T_max = 96
2.806¹¹ - 3.164¹¹
30°
13.6%
1.413¹¹ - 1.597¹¹
60°
12.8%
1.208¹¹ - 1.387¹¹
90°
14.6%
5.296¹¹ - 5.753¹¹
0°
8.6%
Δt = 3,9
T_min = 24
T_max = 96
PERCENTAGE EVALUATION BASED ON F(T_max,Δt_1)
ERROR BARS DETERMINED BY MINIMUM
MODEL-UNCERTAINITY-FACTOR OF 2,
APPLIED TO F (T_max,Δt_1)
CORRESPONDING PROTON VALUES OF |D*| % □

Figure 8

POLAR VS. EQUATORIAL ORBITS: EFFECT OF STEPSIZE ON O.I. FLUXES

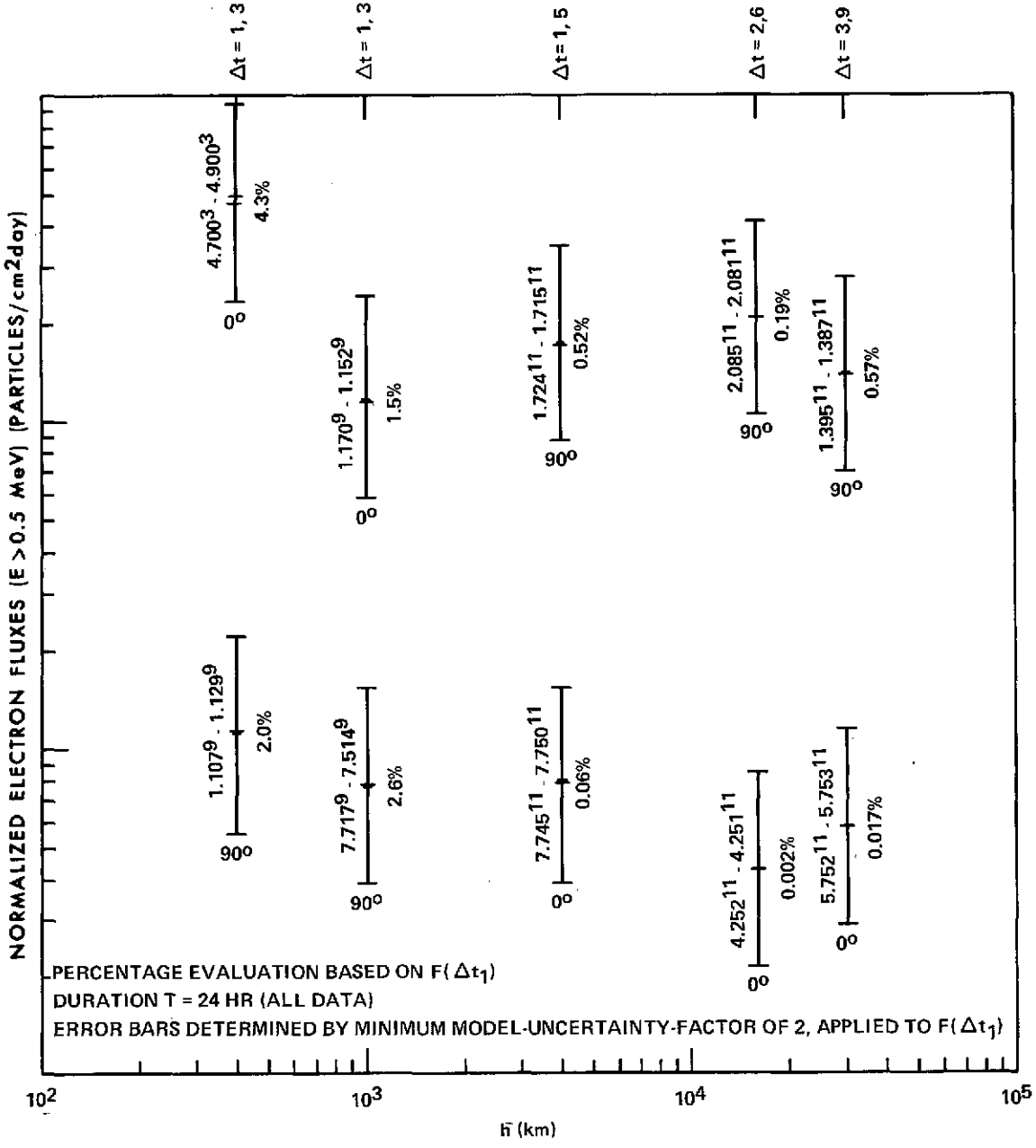

Figure 9

OPTIMAL INTEGRATION CONDITIONS

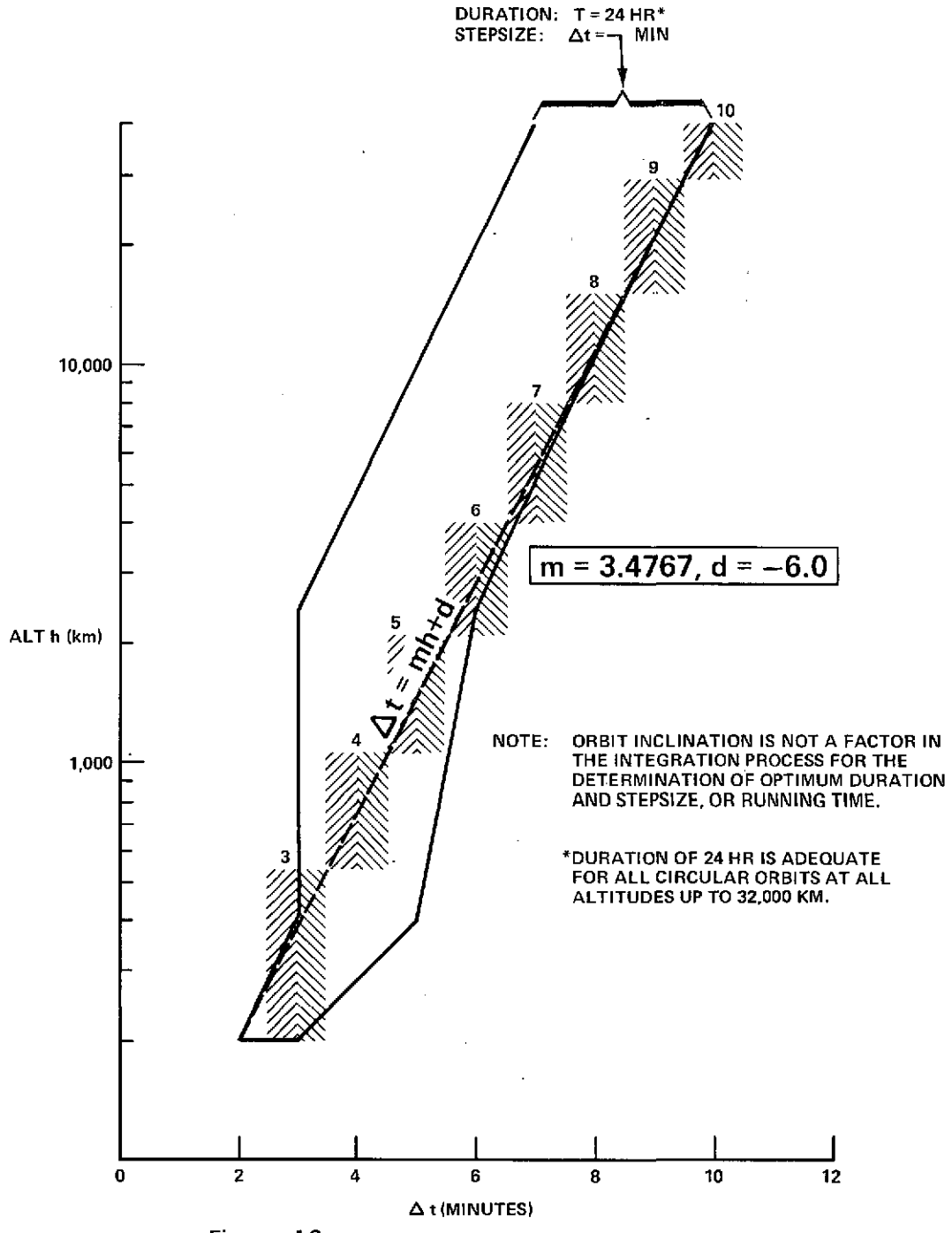

Figure 10

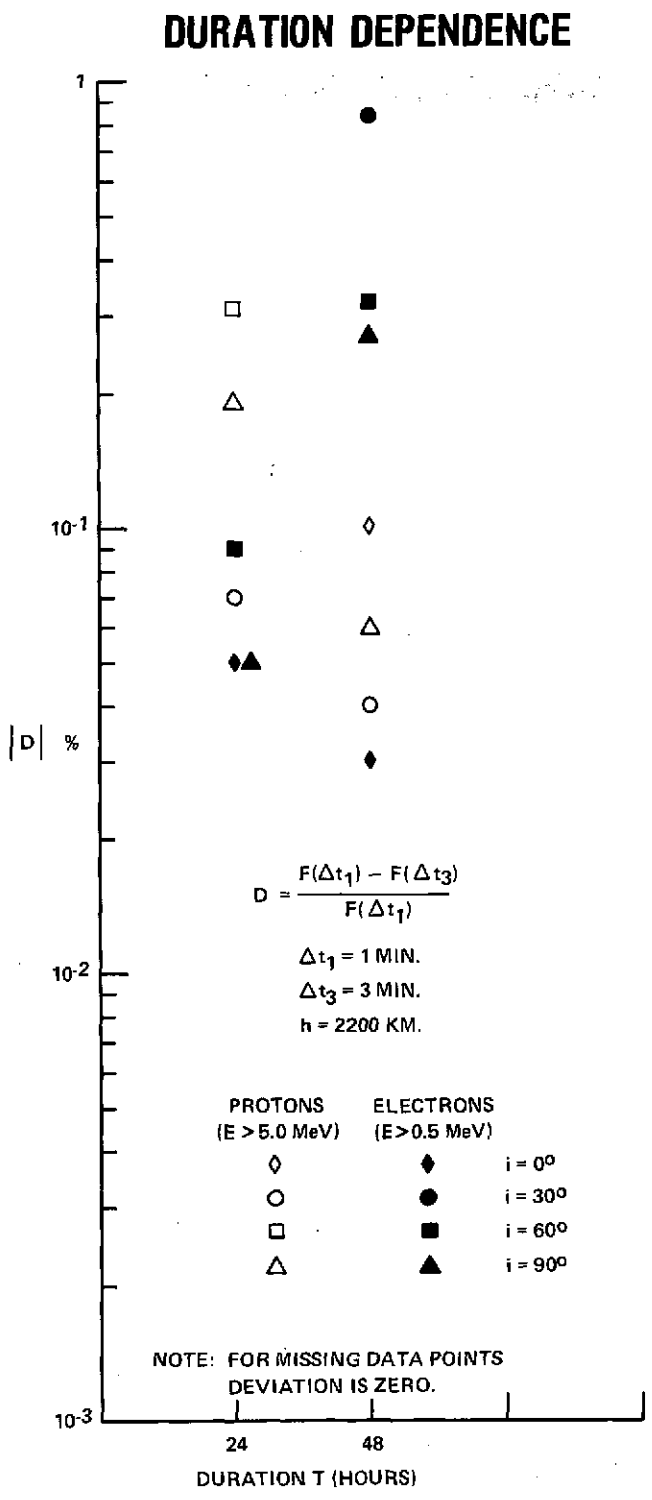
DURATION DEPENDENCE
1
10^{-1}
10^{-2}
10^{-3}
|D| %
$D = \frac{F(\Delta t_1) - F(\Delta t_3)}{F(\Delta t_1)}$
Δt_1 = 1 MIN.
Δt_3 = 3 MIN.
h = 2200 KM.
PROTONS (E > 5.0 MeV)
ELECTRONS (E>0.5 MeV)
i = 0°
i = 30°
i = 60°
i = 90°
NOTE: FOR MISSING DATA POINTS DEVIATION IS ZERO.
24
48
DURATION T (HOURS)

Figure 11

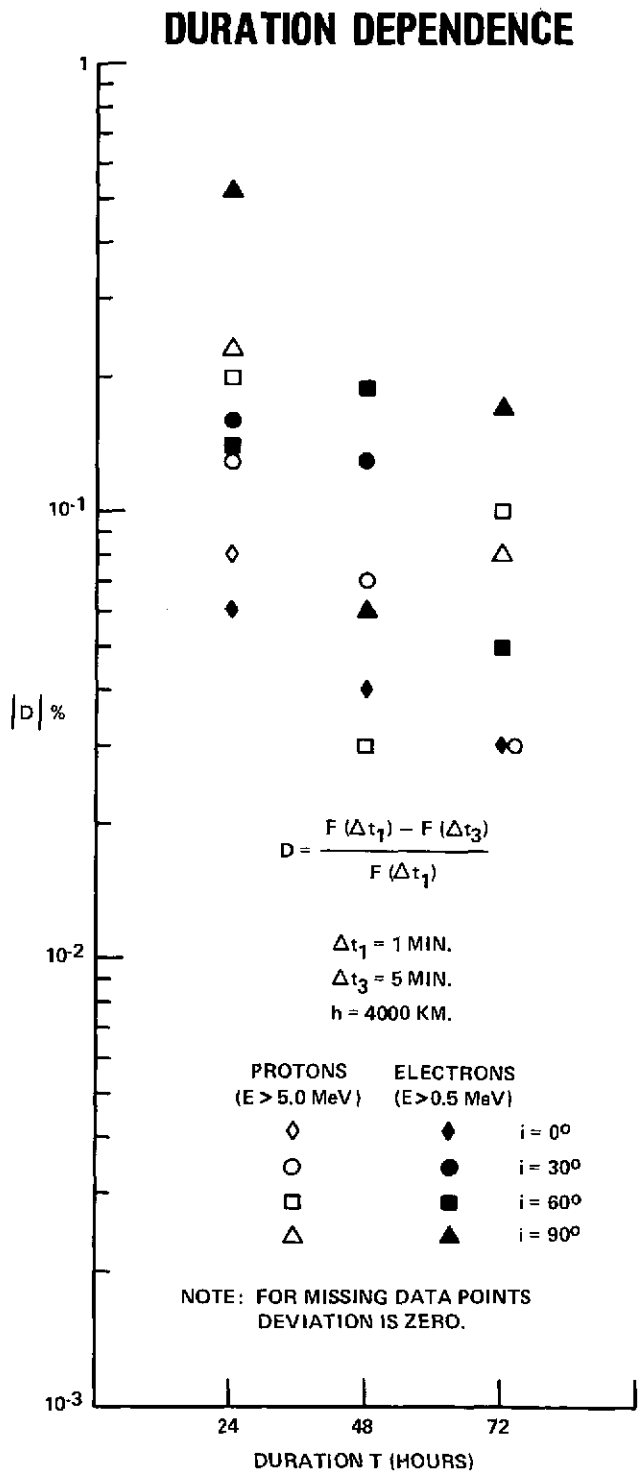
DURATION DEPENDENCE
1
10^{-1}
10^{-2}
10^{-3}
|D| %
$D = \frac{F(\Delta t_1) - F(\Delta t_3)}{F(\Delta t_1)}$
Δt_1 = 1 MIN.
Δt_3 = 5 MIN.
h = 4000 KM.
PROTONS (E > 5.0 MeV)
ELECTRONS (E>0.5 MeV)
i = 0°
i = 30°
i = 60°
i = 90°
NOTE: FOR MISSING DATA POINTS DEVIATION IS ZERO.
24
48
72
DURATION T (HOURS)

Figure 12

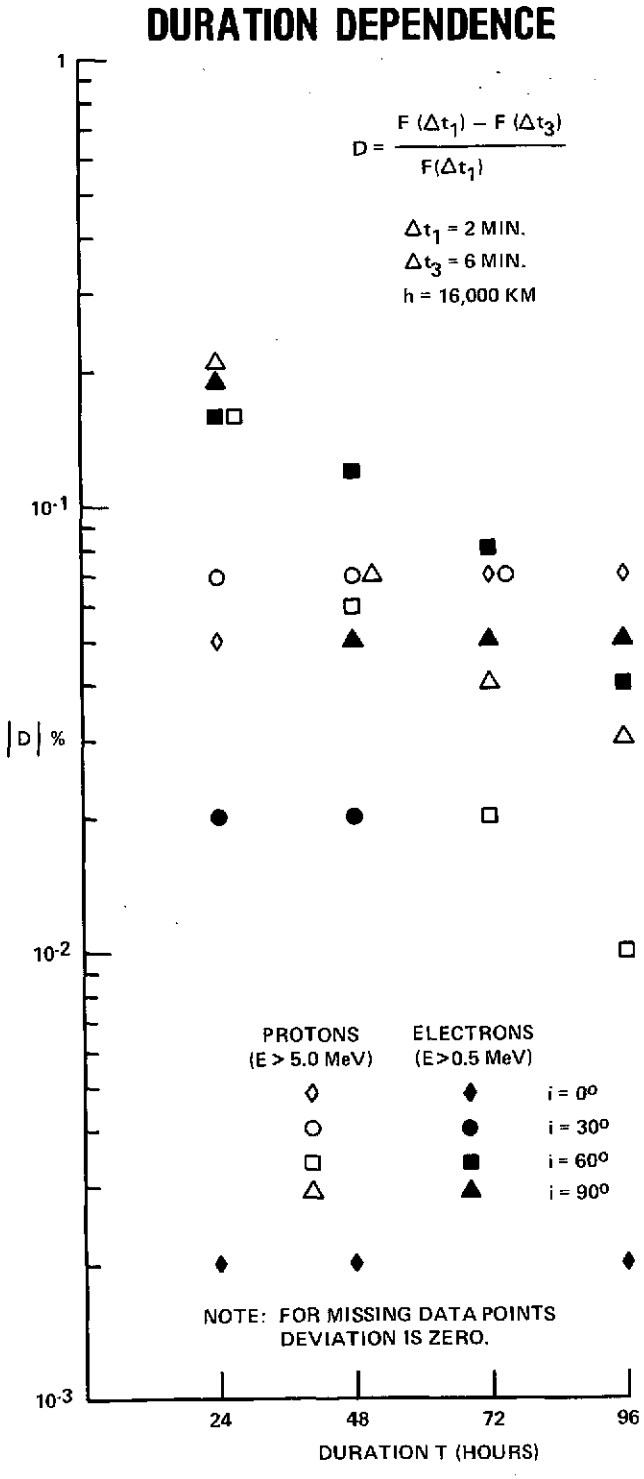
DURATION DEPENDENCE
1
$D = \frac{F(\Delta t_1) - F(\Delta t_3)}{F(\Delta t_1)}$
Δt_1 = 2 MIN.
Δt_3 = 6 MIN.
h = 16,000 KM
10^{-1}
|D| %
10^{-2}
10^{-3}
PROTONS (E > 5.0 MeV)
ELECTRONS (E>0.5 MeV)
i = 0°
i = 30°
i = 60°
i = 90°
NOTE: FOR MISSING DATA POINTS DEVIATION IS ZERO.
24
48
72
96
DURATION T (HOURS)

Figure 13

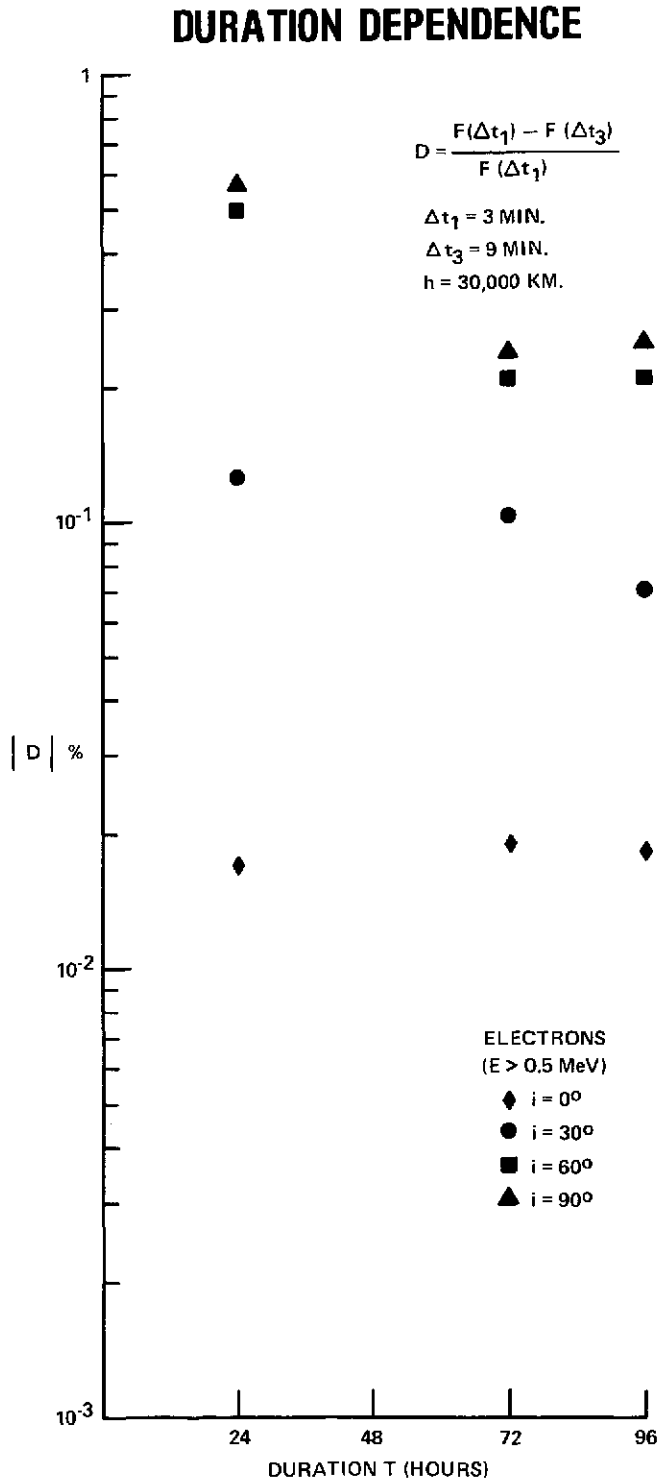
DURATION DEPENDENCE
1
10^{-1}
10^{-2}
10^{-3}
$D = \frac{F(\Delta t_1) - F(\Delta t_3)}{F(\Delta t_1)}$
Δt_1 = 3 MIN.
Δt_3 = 9 MIN.
h = 30,000 KM.
| D | %
ELECTRONS
(E > 0.5 MeV)
i = 0°
i = 30°
i = 60°
i = 90°
24
48
72
96
DURATION T (HOURS)

Figure 14

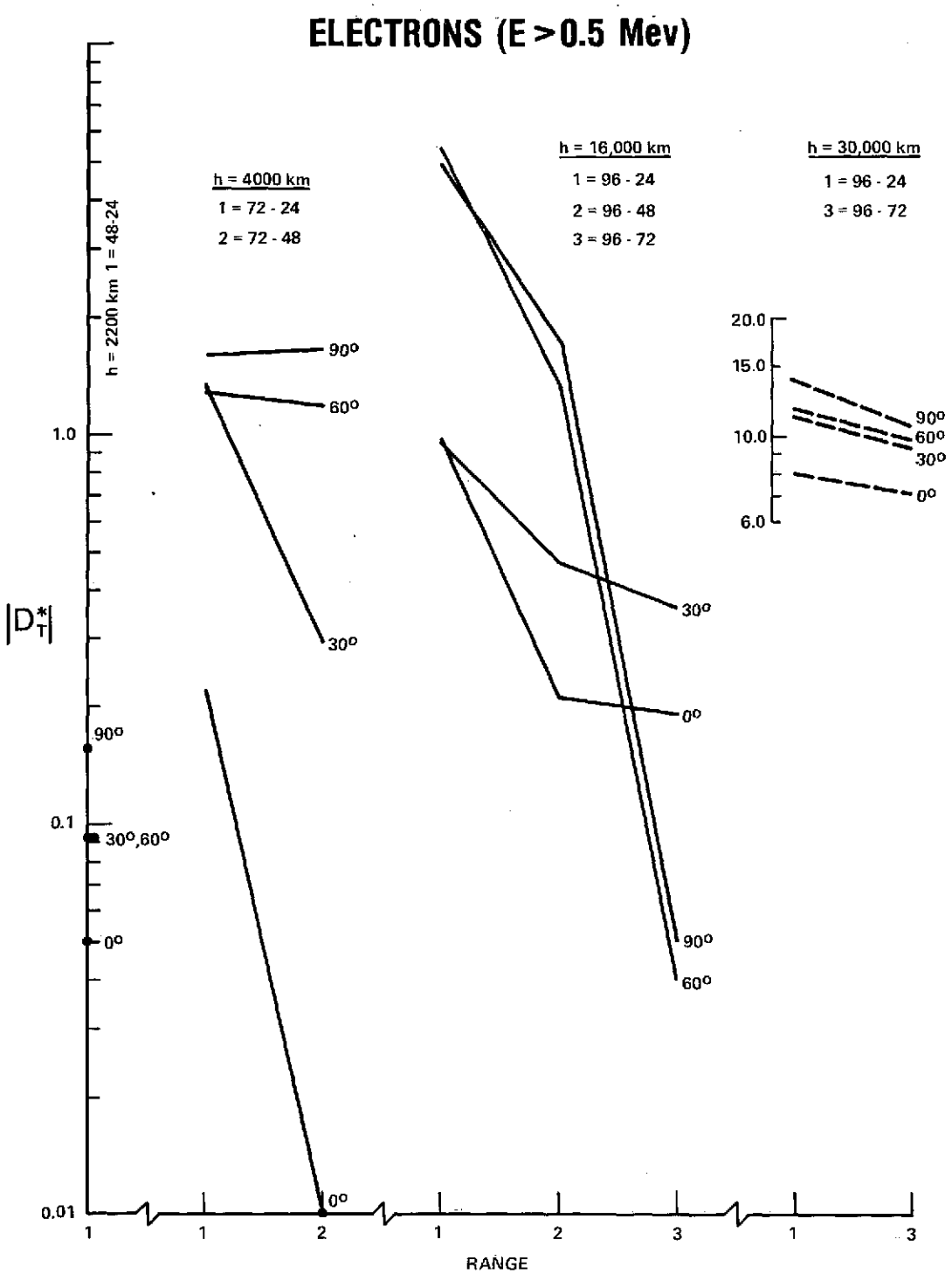
ELECTRONS (E > 0.5 Mev)
h = 4000 km
1 = 72 - 24
2 = 72 - 48
h = 16,000 km
1 = 96 - 24
2 = 96 - 48
3 = 96 - 72
h = 30,000 km
1 = 96 - 24
3 = 96 - 72
h = 2200 km 1 = 48-24
|D*T|
1.0
0.1
0.01
90°
60°
30°
0°
30°,60°
20.0
15.0
10.0
6.0
1
1
2
1
2
3
1
3
RANGE

Figure 15

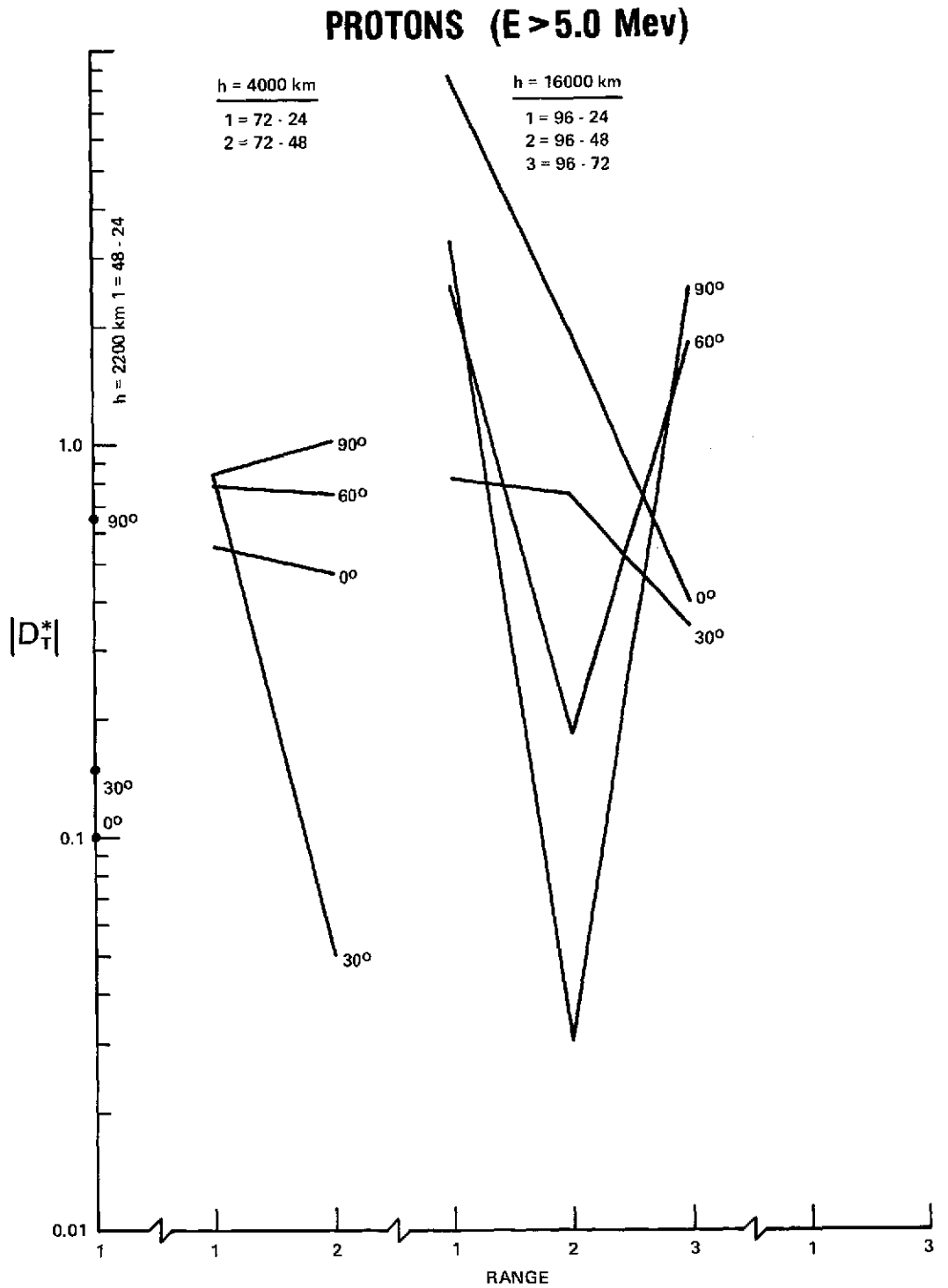
PROTONS (E > 5.0 Mev)
h = 4000 km
1 = 72 - 24
2 = 72 - 48
h = 16000 km
1 = 96 - 24
2 = 96 - 48
3 = 96 - 72
h = 2200 km 1 = 48 - 24
90°
60°
0°
30°
90°
60°
0°
30°
90°
30°
0°
1.0
0.1
0.01
$|D_T^*|$
1
1
2
1
2
3
1
3
RANGE

Figure 16

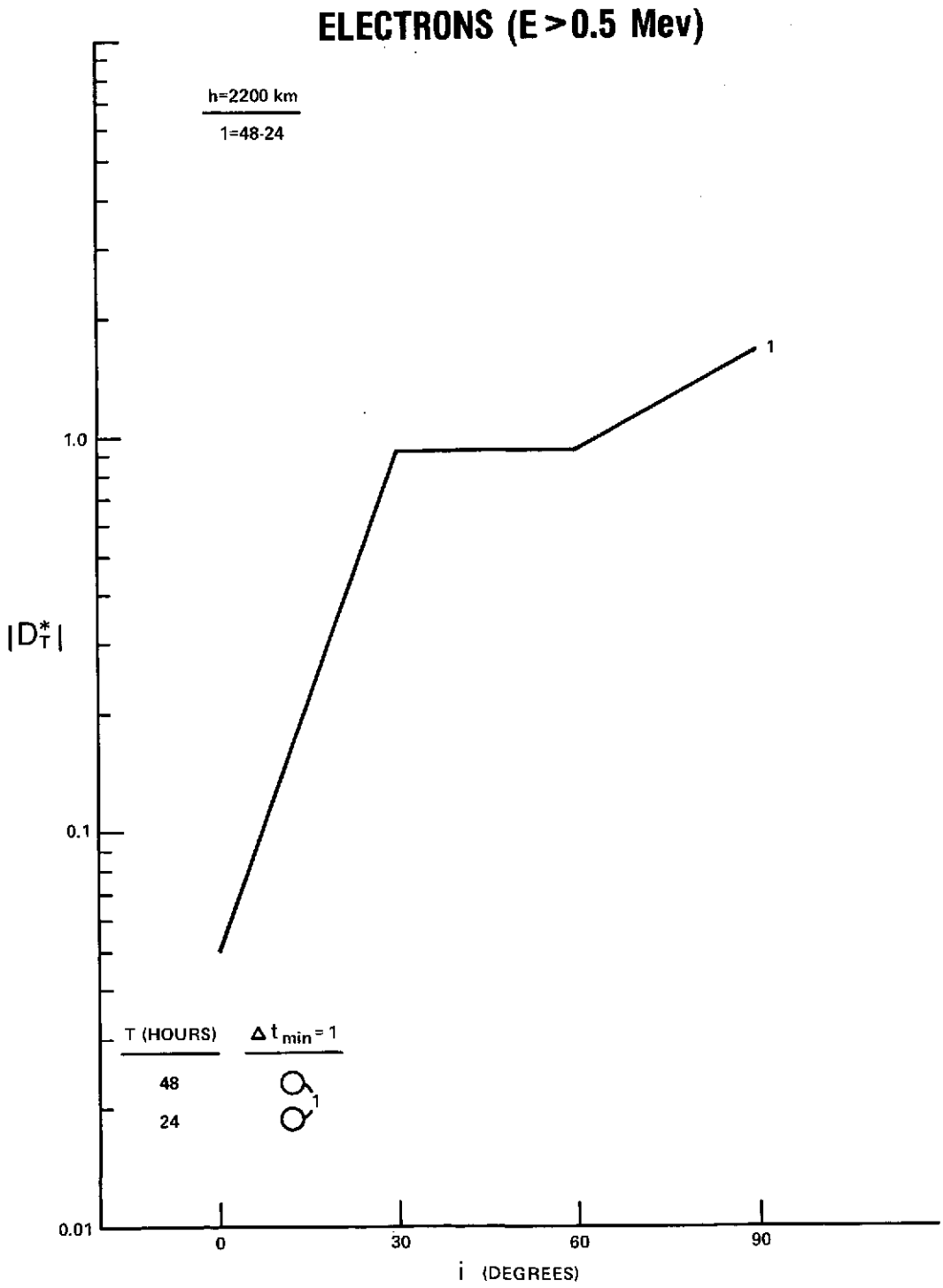
ELECTRONS (E > 0.5 Mev)
h=2200 km
1=48-24
1
1.0
0.1
0.01
|D*T|
T (HOURS)
Δ t min = 1
48
24
1
0
30
60
90
i (DEGREES)

Figure 17

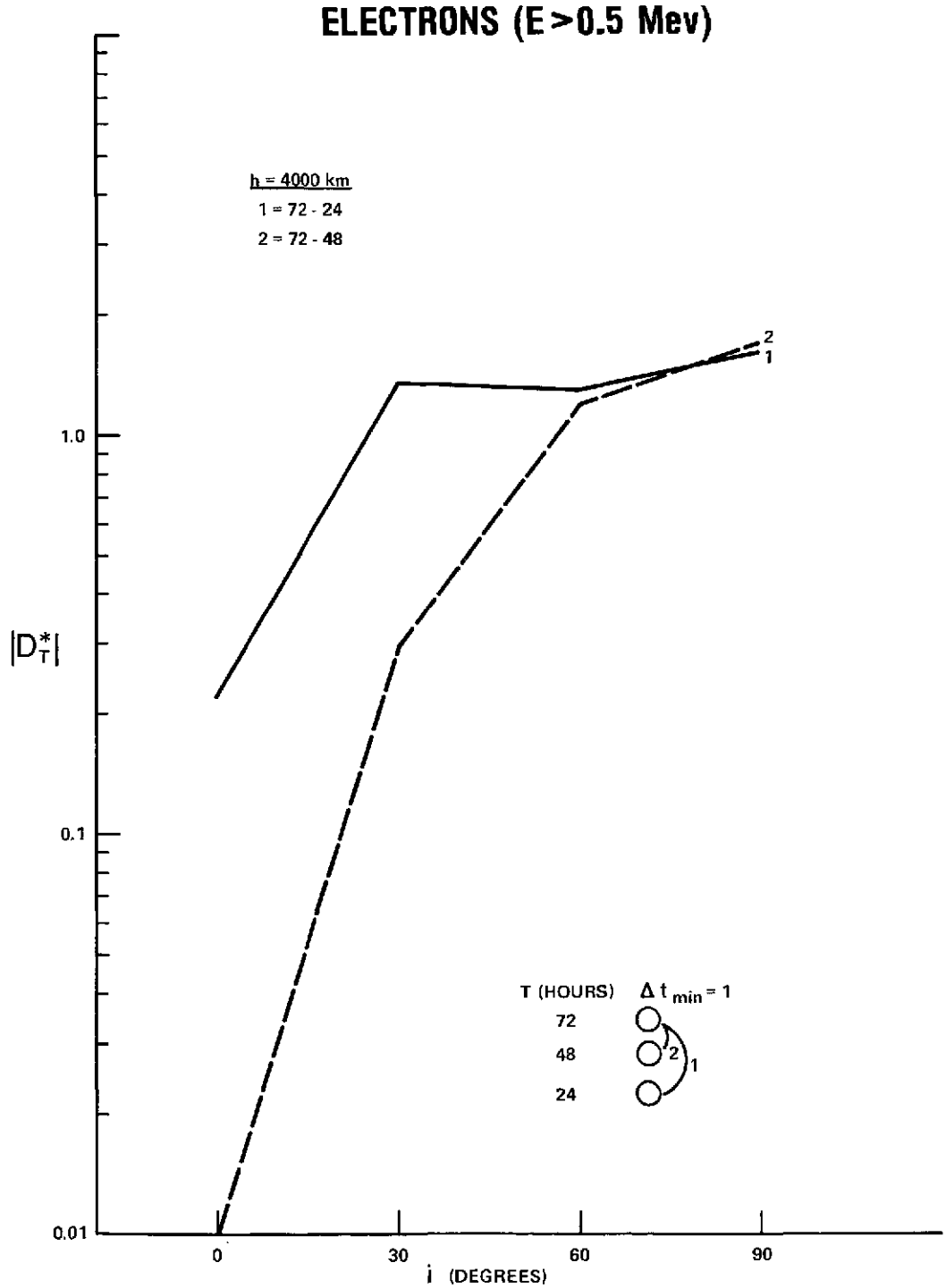
ELECTRONS (E>0.5 Mev)
h = 4000 km
1 = 72 - 24
2 = 72 - 48
1.0
0.1
0.01
$|D_T^*|$
0
30
60
90
i (DEGREES)
T (HOURS)
$\Delta t_{min} = 1$
72
48
24
2
1

Figure 18

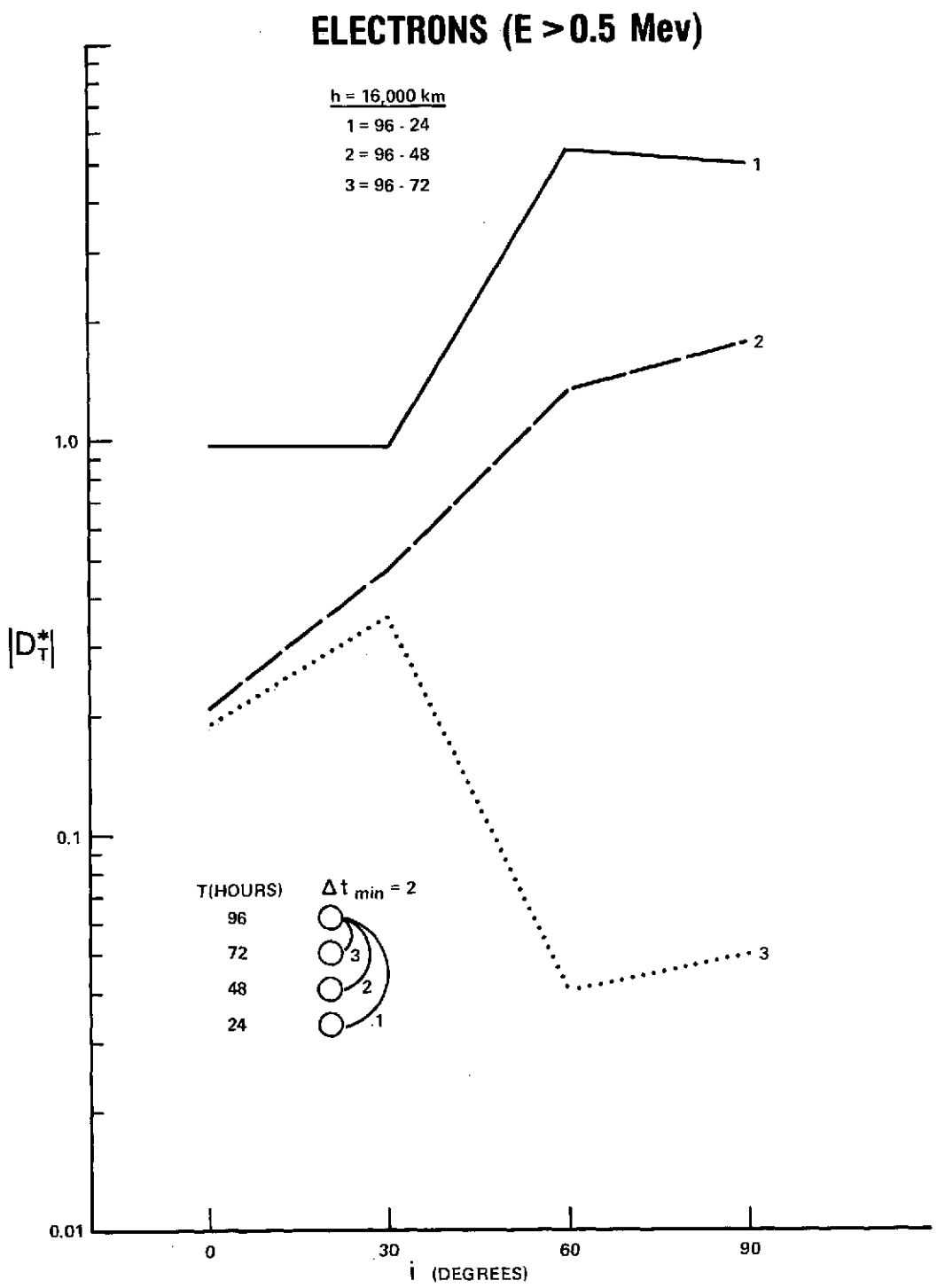
ELECTRONS (E > 0.5 Mev)
h = 16,000 km
1 = 96 - 24
2 = 96 - 48
3 = 96 - 72
1
2
3
1.0
0.1
0.01
$|D_T^*|$
T(HOURS)
$\Delta t_{min} = 2$
96
72
48
24
0
30
60
90
i (DEGREES)

Figure 19

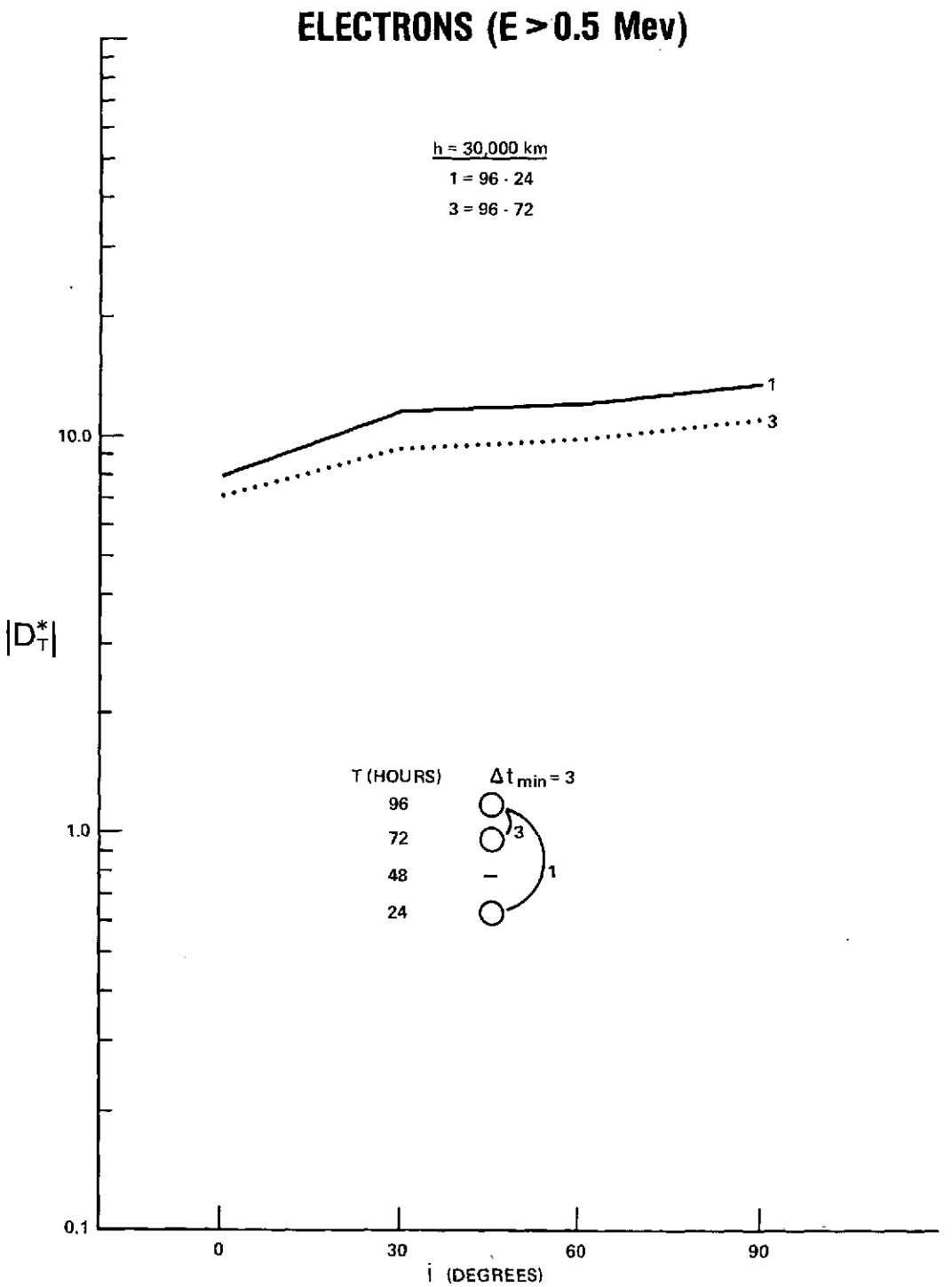
ELECTRONS (E > 0.5 Mev)
h = 30,000 km
1 = 96 - 24
3 = 96 - 72
10.0
1.0
0.1
|D*T|
1
3
T (HOURS)
Δt min = 3
96
72
48
24
3
1
0
30
60
90
i (DEGREES)

Figure 20

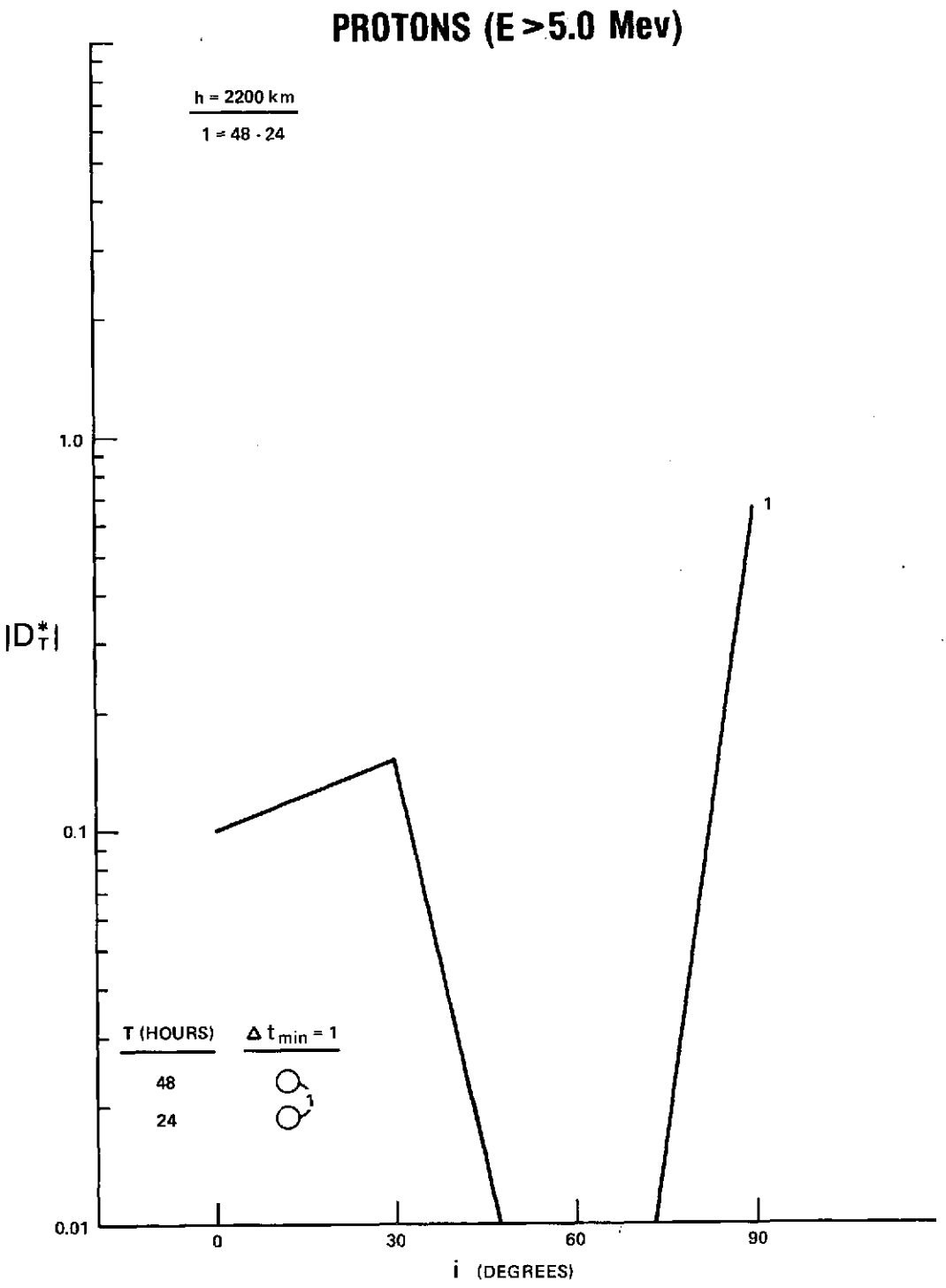
PROTONS (E >5.0 Mev)
h = 2200 km
1 = 48 - 24
1.0
0.1
0.01
|D*T|
1
T (HOURS)
Δ tmin = 1
48
24
1
0
30
60
90
i (DEGREES)

Figure 21

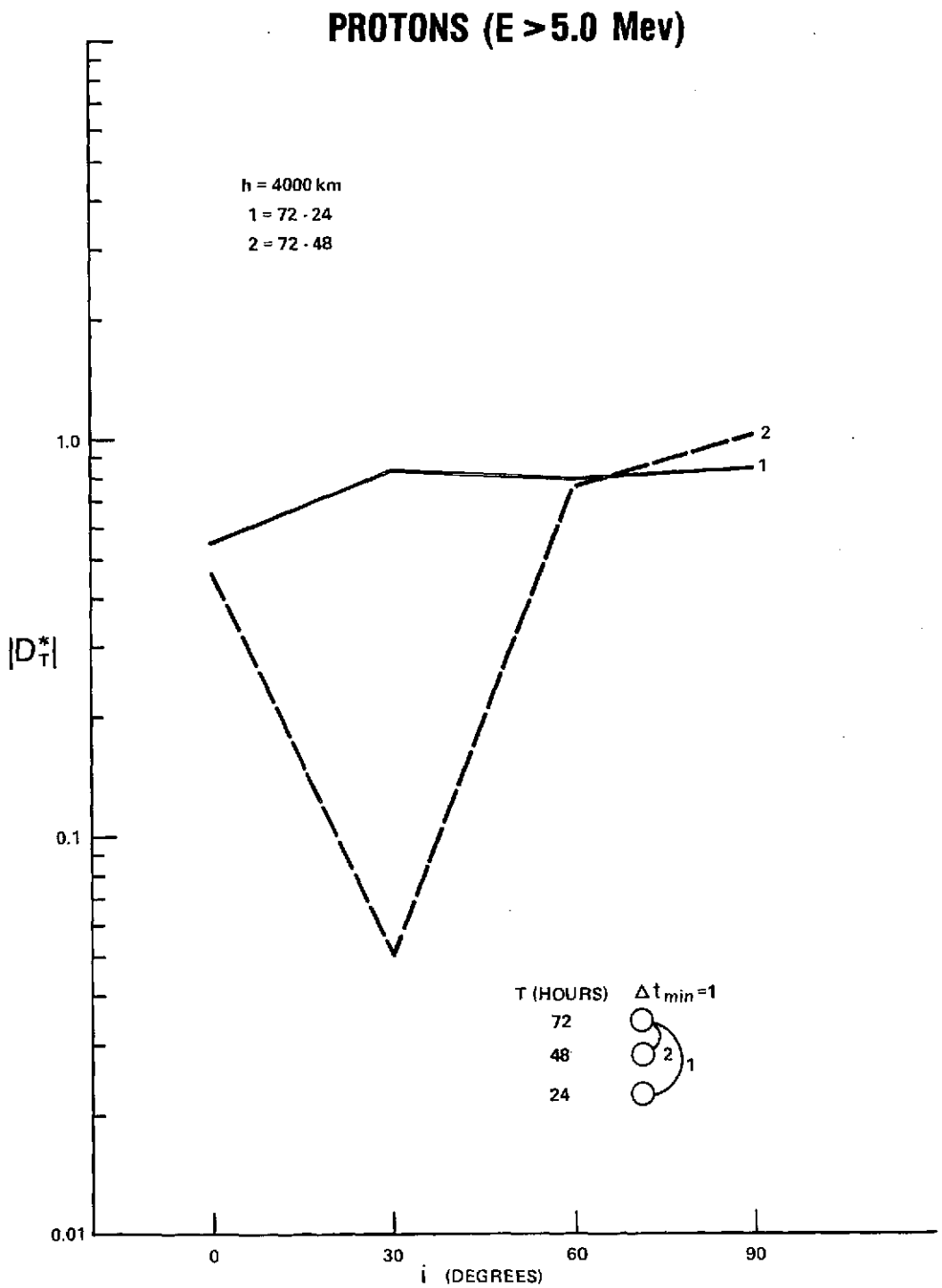
PROTONS (E >5.0 Mev)
h = 4000 km
1 = 72 - 24
2 = 72 - 48
1.0
0.1
0.01
|D*T|
2
1
T (HOURS)
Δt min =1
72
48
24
2
1
0
30
60
90
i (DEGREES)

Figure 22

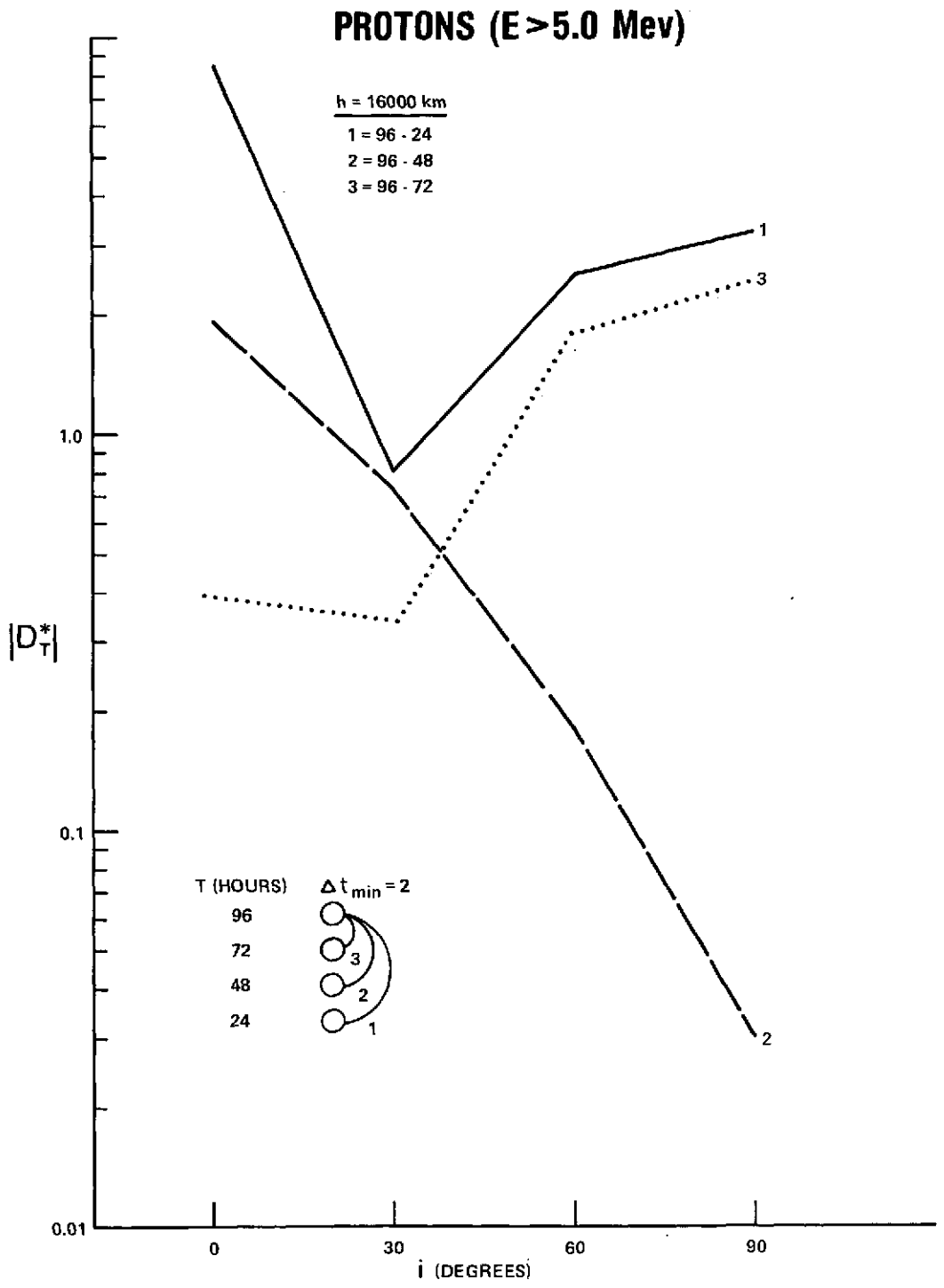
PROTONS (E>5.0 Mev)
h = 16000 km
1 = 96 - 24
2 = 96 - 48
3 = 96 - 72
1
3
2
1.0
0.1
0.01
$|D_T^*|$
T (HOURS)
$\Delta t_{min} = 2$
96
72
48
24
0
30
60
90
i (DEGREES)

Figure 23

DETERMINATION OF OPTIMAL INTEGRATION CONDITIONS: TEST RESULTS

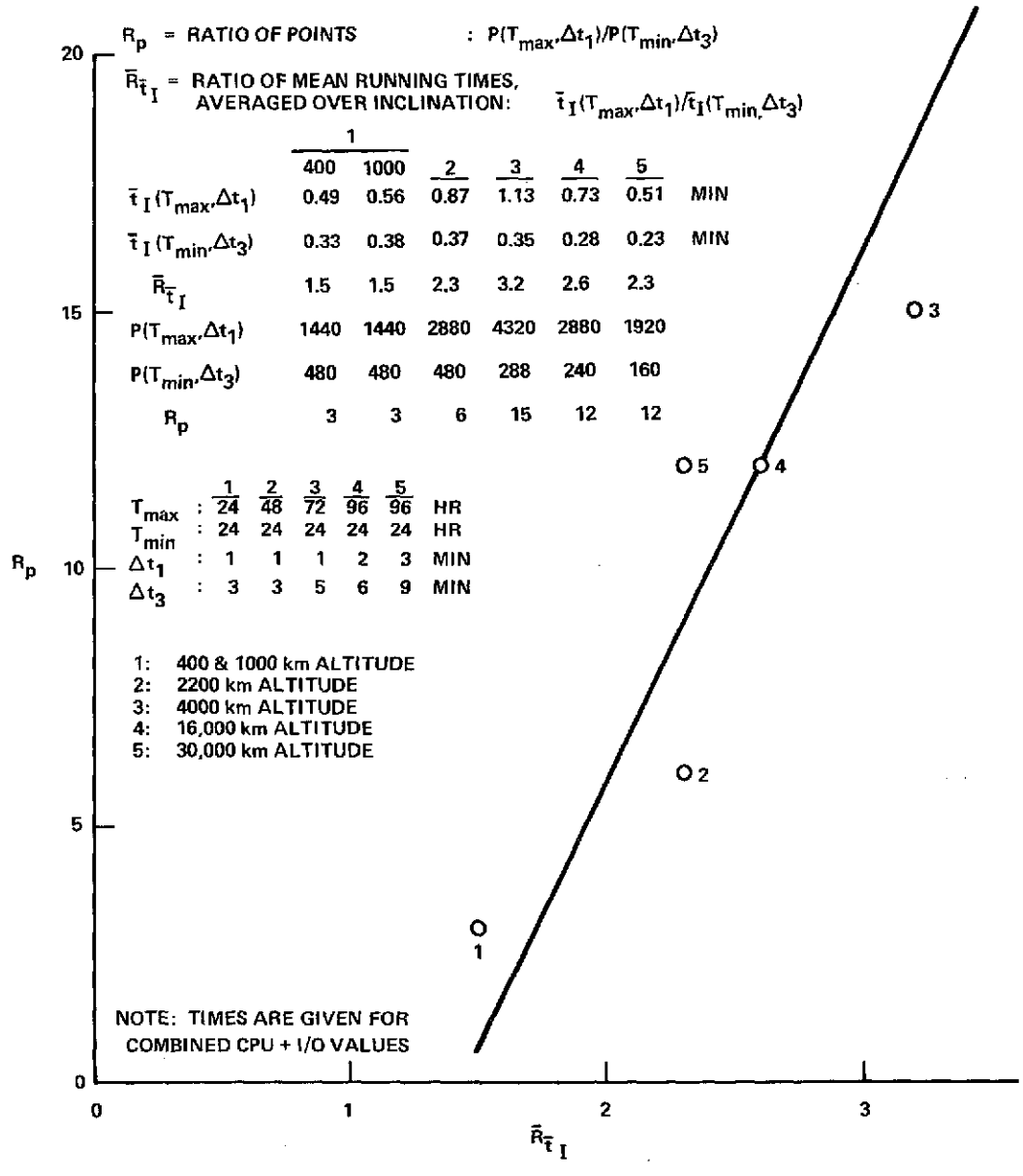

	1		2	3	4	5	
	400	1000					
$\bar{t}_I(T_{max},\Delta t_1)$	0.49	0.56	0.87	1.13	0.73	0.51	MIN
$\bar{t}_I(T_{min},\Delta t_3)$	0.33	0.38	0.37	0.35	0.28	0.23	MIN
$\bar{R}_{\bar{t}_I}$	1.5	1.5	2.3	3.2	2.6	2.3	
$P(T_{max},\Delta t_1)$	1440	1440	2880	4320	2880	1920	
$P(T_{min},\Delta t_3)$	480	480	480	288	240	160	
R_p	3	3	6	15	12	12	

	1	2	3	4	5	
T_{max} :	24	48	72	96	96	HR
T_{min} :	24	24	24	24	24	HR
Δt_1 :	1	1	1	2	3	MIN
Δt_3 :	3	3	5	6	9	MIN

Figure 24

INCLINATION AVERAGED RUNNING TIMES: COMBINED CPU & I/O OF EXECUTION STEP

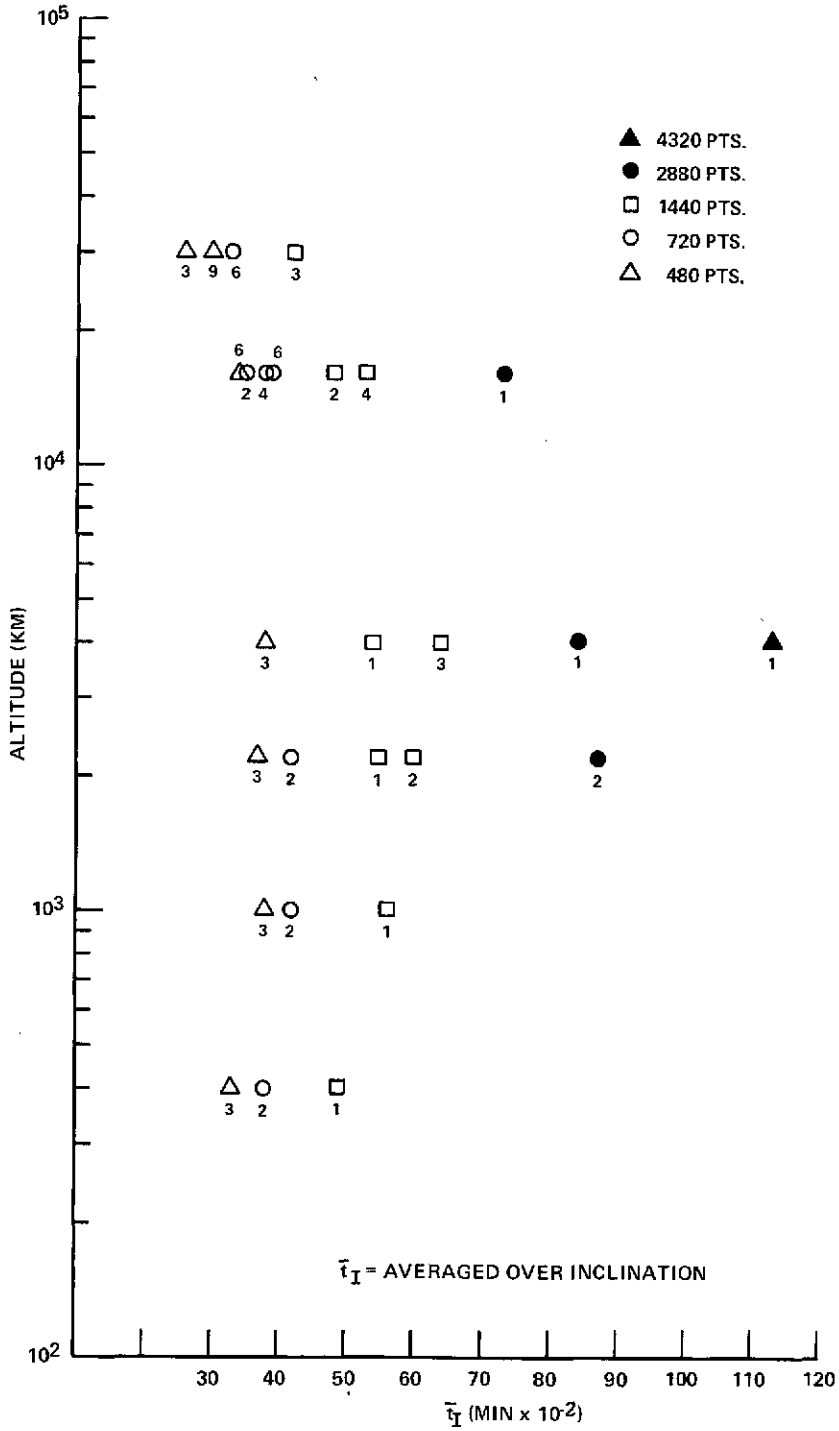

Figure 25

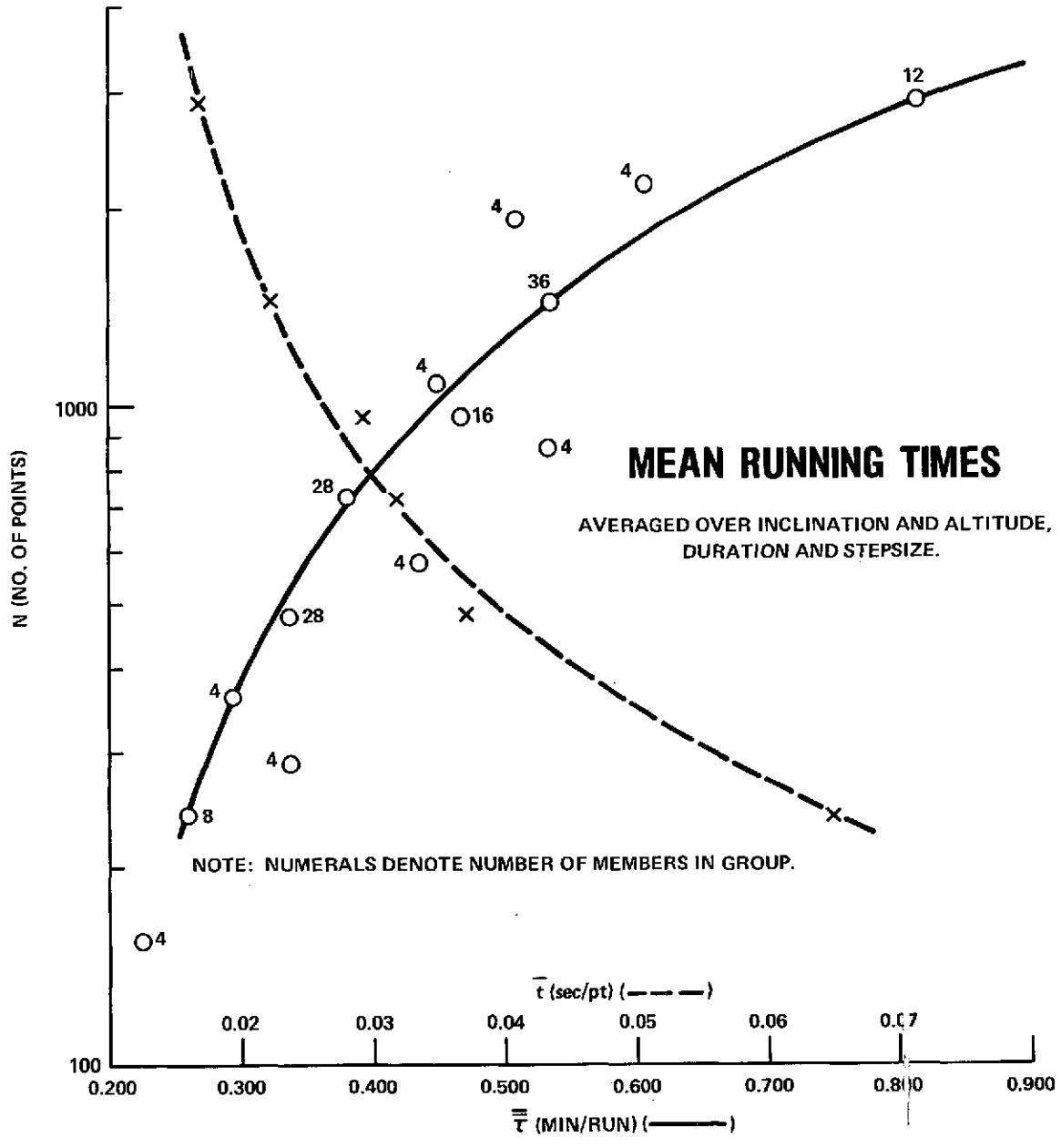
MEAN RUNNING TIMES
AVERAGED OVER INCLINATION AND ALTITUDE, DURATION AND STEPSIZE.
NOTE: NUMERALS DENOTE NUMBER OF MEMBERS IN GROUP.
N (NO. OF POINTS)
1000
100
t (sec/pt) (— — —)
0.02
0.03
0.04
0.05
0.06
0.07
0.200
0.300
0.400
0.500
0.600
0.700
0.800
0.900
τ (MIN/RUN) (———)
12
36
16
28
8
4

Figure 26